Cell Host & Microbe
Article

The Classical Lancefield Antigen of Group A *Streptococcus* Is a Virulence Determinant with Implications for Vaccine Design

Nina M. van Sorge,[1,6,15,*] Jason N. Cole,[1,7,15] Kirsten Kuipers,[1] Anna Henningham,[1,7] Ramy K. Aziz,[2,8] Ana Kasirer-Friede,[3] Leo Lin,[1] Evelien T.M. Berends,[6] Mark R. Davies,[7,9] Gordon Dougan,[9] Fan Zhang,[10] Samira Dahesh,[1] Laura Shaw,[1] Jennifer Gin,[4] Madeleine Cunningham,[11] Joseph A. Merriman,[12] Julia Hütter,[13,14] Bernd Lepenies,[13,14] Suzan H.M. Rooijakkers,[6] Richard Malley,[10] Mark J. Walker,[7] Sanford J. Shattil,[3] Patrick M. Schlievert,[12] Biswa Choudhury,[5] and Victor Nizet[1,4,5,*]
[1]Department of Pediatrics
[2]Department of Bioengineering
[3]Department of Medicine
[4]Skaggs School of Pharmacy and Pharmaceutical Sciences
[5]Glycobiology Research and Training Center
University of California, San Diego, La Jolla, CA 92093, USA
[6]Medical Microbiology, University Medical Center Utrecht, 3584 CX Utrecht, The Netherlands
[7]Australian Infectious Diseases Research Centre, School of Chemistry and Molecular Biosciences, The University of Queensland, St. Lucia, Queensland, QLD 4072, Australia
[8]Department of Microbiology and Immunology, Faculty of Pharmacy, Cairo University, 11562 Cairo, Egypt
[9]The Wellcome Trust Sanger Institute, The Wellcome Trust Genome Campus, Hinxton CB10 1SA, UK
[10]Division of Infectious Diseases, Boston Children's Hospital, Boston, MA 02115, USA
[11]Department of Microbiology and Immunology, University of Oklahoma Health Sciences Center, Oklahoma City, OK 73104, USA
[12]Department of Microbiology, Carver College of Medicine, University of Iowa, Iowa City, IA 52242, USA
[13]Max Planck Institute of Colloids and Interfaces, Department of Biomolecular Systems, 14476 Potsdam, Germany
[14]Freie Universität Berlin, Institute of Chemistry and Biochemistry, Department of Biology, Chemistry and Pharmacy, 14195 Berlin, Germany
[15]Co-first author
*Correspondence: n.vansorge-3@umcutrecht.nl (N.M.v.S.), vnizet@ucsd.edu (V.N.)
http://dx.doi.org/10.1016/j.chom.2014.05.009

SUMMARY

Group A *Streptococcus* (GAS) is a leading cause of infection-related mortality in humans. All GAS serotypes express the Lancefield group A carbohydrate (GAC), comprising a polyrhamnose backbone with an immunodominant *N*-acetylglucosamine (GlcNAc) side chain, which is the basis of rapid diagnostic tests. No biological function has been attributed to this conserved antigen. Here we identify and characterize the GAC biosynthesis genes, *gacA* through *gacL*. An isogenic mutant of the glycosyltransferase *gacI*, which is defective for GlcNAc side-chain addition, is attenuated for virulence in two infection models, in association with increased sensitivity to neutrophil killing, platelet-derived antimicrobials in serum, and the cathelicidin antimicrobial peptide LL-37. Antibodies to GAC lacking the GlcNAc side chain and containing only polyrhamnose promoted opsonophagocytic killing of multiple GAS serotypes and protected against systemic GAS challenge after passive immunization. Thus, the Lancefield antigen plays a functional role in GAS pathogenesis, and a deeper understanding of this unique polysaccharide has implications for vaccine development.

INTRODUCTION

Streptococcus pyogenes, commonly known as group A *Streptococcus* (GAS), is a preeminent human pathogen responsible for ~700 million cases of pharyngitis ("strep throat") annually worldwide and increasing numbers of severe invasive infections, including necrotizing fasciitis ("flesh-eating disease") and streptococcal toxic shock syndrome (Carapetis et al., 2005). GAS is also responsible for the postinfectious immune-mediated disease rheumatic fever, which is a major cause of chronic heart disease and mortality in many parts of the developing world (Carapetis et al., 2005; Marijon et al., 2012). Serological classification of streptococci in groups is based upon expression of unique carbohydrate antigens in the bacterial cell wall (Lancefield, 1928), known only to play a structural role in cell wall biogenesis (Caliot et al., 2012; McCarty, 1952). All serotypes of GAS express the Lancefield group A carbohydrate (GAC), comprising a polyrhamnose backbone with an immunodominant *N*-acetylglucosamine (GlcNAc) side chain (McCarty, 1952, 1956); this GlcNAc epitope of GAC is the basis of all rapid diagnostic testing for GAS infection. Remarkably, ~50% of the GAS cell wall by weight is made up of the GAC (McCarty, 1952); however, a specific biological function has yet to be attributed to this conserved and abundant eponymous antigen.

Despite a high global demand (Carapetis et al., 2005), there is currently no safe and efficacious commercial vaccine against GAS infection. Certain unique phenotypic features of the pathogen pose particular challenges to vaccination (Pandey et al.,

2012), including the invariant GAS capsule composed of hyaluronic acid (Kendall et al., 1937), an immunologically inert carbohydrate ubiquitous in human connective tissues. In addition, immunodominant surface-anchored GAS M proteins are polymorphic (>200 *emm* genotypes) (McMillan et al., 2013), and regions of their dimeric coiled-coil structure may provoke an autoimmune response against cardiac tissue in rheumatic fever (Faé et al., 2005). Due to its prominence in the GAS cell wall and its conservation across all GAS serotypes, the GAC has been considered as a potential antigen for a universal GAS vaccine. Passive and active mouse immunization studies with protein conjugate vaccines using purified or synthetic versions of the wild-type (WT) GAC show significant efficacy against multiple GAS serotypes (Kabanova et al., 2010; Sabharwal et al., 2006). Moreover, anti-GAC antibodies are detected in human serum; high titers correlate with decreased colonization in children (Sabharwal et al., 2006) and peak around age 17, correlating with dropping GAS infection rates after this age (Zimmerman et al., 1971). However, theoretical concerns regarding autoreactivity of antibodies that recognize the native GAC GlcNAc side chain against human tissues have been raised by several groups, but remain a point of significant controversy. Glycoproteins from human heart valves, when used to immunize rabbits, engender antibodies that bind to GAC in a manner inhibited by GlcNAc (but not rhamnose and other sugars) (Goldstein et al., 1968), and persistence of anti-GlcNAc/GAC antibodies (from 1 to 20 years) are a marker of poor prognosis of heart valve problems in rheumatic heart disease (RHD), whereas antibodies against streptolysin O and the polyrhamnose core of GAC decline independently of valve complications (Ayoub et al., 1974; Dudding and Ayoub, 1968; Shulman et al., 1974). The specificity and persistence of elevated anti-GAC (GlcNAc) antibody titers for rheumatic mitral valve heart disease was also suggested in a study of 30 patients versus equal-sized control groups of control individuals, patients with congenital heart disease, and patients with nonrheumatic mitral valve prolapse (Appleton et al., 1985). Finally, anti-GlcNAc monoclonal antibodies, cross-reactive for heart or brain tissue, have been derived from patients with rheumatic fever and its cardiac or neurological complications (Galvin et al., 2000; Kirvan et al., 2003).

Here, we identify the genes responsible for GAC biosynthesis, identify a role for the GlcNAc side chain in GAS resistance to host innate immunity, and discuss potential implications of this new genetic insight for GAS vaccine design.

RESULTS

Identification and Mutagenesis of GAC Biosynthesis Genes *gacA* through *gacL*

Analogous to a bioinformatic analysis of group B *Streptococcus* (GBS) (Sutcliffe et al., 2008), we searched the GAS chromosome for clusters enriched in genes encoding rhamnose polysaccharide-related proteins and identified a putative 12-gene GAC biosynthesis locus (Figure 1A) that is completely conserved among all sequenced GAS genomes published to date. Many of these genes, herein designated *gacABCDEFGHIJKL*, are predicted to encode proteins with functional annotations as glycosyltransferases (including rhamnosyltransferases) and polysaccharide transport proteins (Figure 1A). The same 12-gene *gacA–gacL* cluster was identified in a 16 kb nonhomologous region in two *Streptococcus dysgalactiae* subsp. *equisimilis* (SDSE) strains from invasive human infections, which typically express group C or G carbohydrate antigens, but showed unexpected reactivity to the GAS latex agglutination test (McMillan et al., 2010) (Figures 2A–2C), implying a recent recombination event between GAS and a progenitor to the SDSE strains. Similar "hybrid strains" have been described, but a genetic basis has never been identified (Tanaka et al., 2008). Using a representative strain of the globally disseminated serotype M1T1 GAS clone (5448), we performed a plasmid integrational mutagenesis scan across the gene cluster. Nine of 12 mutants (targeting genes *gacD–gacL*) were viable. Three of nine mutants (disrupting *gacI*, *gacJ*, and *gacK*) lost reactivity in the diagnostic GAS latex agglutination test (Figure 1B) and no longer interacted with a GlcNAc-specific lectin, succinylated wheat germ agglutinin (sWGA) (Figure 1B), indicating loss of the hallmark side chain. Normal growth phenotypes were observed for the majority of mutants, except those targeting *gacG* (putative rhamnosyltransferase), which reached lower stationary phase optical density, and *gacJ* (annotated only as a membrane protein), which grew only upon addition of 0.5 M sucrose for osmotic stabilization (Figure S1A). Even with osmotic stabilization, we were unable to obtain mutants in *gacA*, predicted to generate activated rhamnose, nor the annotated rhamnosyltransferases *gacB* and *gacC*, suggesting that all three genes are essential for production of the core polyrhamnose backbone.

Glycosyltransferase GacI Is Essential for the Expression of the GAC GlcNAc Side Chain

To study the specific role of the GlcNAc side chain in GAS virulence phenotypes, we generated a precise in-frame allelic replacement mutant eliminating *gacI*, an annotated glycosyltransferase. The ΔGacI mutant lost reactivity in the diagnostic GAS latex agglutination test and interaction with GlcNAc-specific lectin sWGA (Figure 1C); both phenotypes were restored by reintroducing the *gacI* gene (marked with a silent mutation) into the ΔGacI mutant chromosome, yielding the reconstituted strain GacI* (Figure 1C). Extraction and purification of GAC from WT GAS, ΔGacI, and GacI* strains followed by glycan composition and linkage analysis unambiguously confirmed the absence of GlcNAc side chain in the ΔGacI mutant, leaving the polyrhamnose core intact (Figures 1D and 1E; Figures S1B and S1C). Historically, "antigen-negative" GAS strains are known as "A-variant" strains and infrequently arise upon serial passage in mice and rabbits (McCarty and Lancefield, 1955; Wilson, 1945), but have never been isolated from humans, suggesting a crucial role for the side chain in human infection, the only natural host of GAS.

The TarO Homolog GacO Contributes to GAC Biosynthesis

In GBS, a neonatal pathogen, the enzyme encoded by *gbcO* catalyzes the transfer of GlcNAc-1-phosphate to bactoprenyl phosphate and is essential for synthesis of the GBS cell wall carbohydrate (GBC) (Caliot et al., 2012). A GBS *gbcO* knockout mutant lacks cell wall rhamnose, exhibits aberrant cell morphology and slow growth, and has impaired peptidoglycan polymerization leading to mutanolysin hypersensitivity (Caliot et al., 2012); all these phenotypes are reproduced in WT GBS

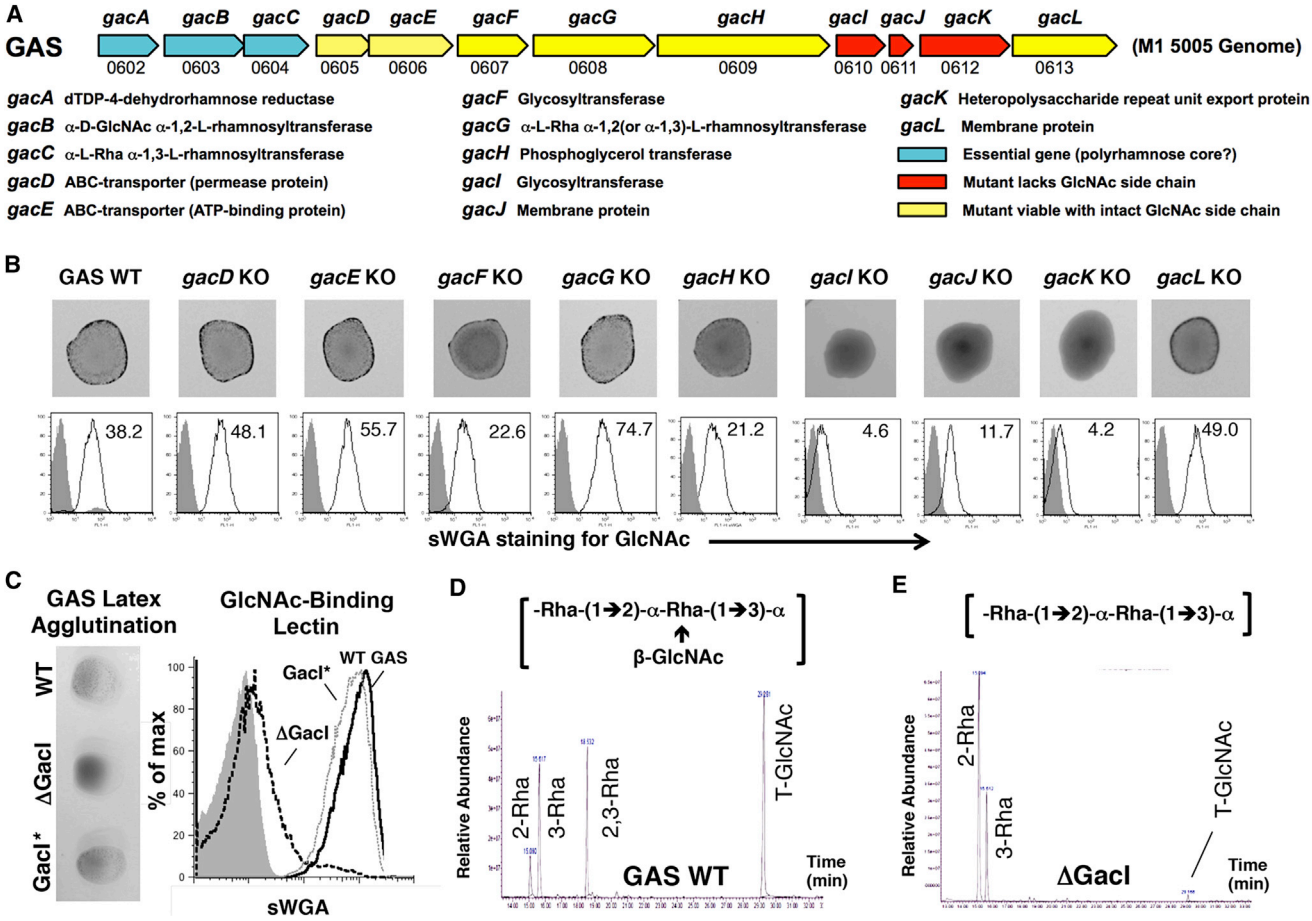

Figure 1. Schematic Representation of the GAC Gene Cluster, Mutagenesis Scan, and ΔGacI Mutant

(A) Schematic representation of the GAS M1T1 strain 5448 group A carbohydrate (GAC) gene cluster M5005_Spy0602-0613, which was renamed *gacA–gacL*, and annotated gene functions based on analysis using the SEED tools (http://pubseed.theseed.org).

(B) Latex agglutination reaction with GAC-specific beads and GlcNAc-specific sWGA lectin staining of viable GAS insertional knockout mutants in genes *gacD–gacL*. Gray fill, medium control; black line, sWGA-FITC stain. Histogram numbers indicate geometric mean of fluorescence.

(C) Latex agglutination reaction with GAC-specific beads and GlcNAc expression as assessed by sWGA stain as indicated on GAS WT, ΔGacI mutant, and GacI* complemented strain.

(D and E) HPLC tracing and linkage analysis with deduced schematic structure of the repeating unit of extracted GAC from (D) GAS WT and (E) ΔGacI mutant strain. See also Figure S1.

by treatment with tunicamycin (Caliot et al., 2012), a specific inhibitor of *gbcO*-type transferases (Campbell et al., 2011). GAS has a homolog of *gbcO* (MGAS5005_spy0240, *gacO*) located at a distance in the chromosome from the 12-gene locus described here. As was seen with GBS (Caliot et al., 2012), treatment of WT GAS with tunicamycin inhibited growth, increased mutanolysin sensitivity, induced aberrant morphology, and eliminated cell wall rhamnose (Figures 3A–3D), suggesting that *gacO* is essential for synthesis of the GAC polyrhamnose core and bacterial viability. Similar defects in cell wall integrity were not observed with the ΔGacI mutant strain. To assess GAS cell wall integrity in more depth at the functional level, we exposed WT and ΔGacI mutant GAS to stresses that can disrupt a generally weakened cell wall. WT and ΔGacI GAS strains grew at similar rates under high salt (up to 300 mM NaCl) and varying pH (6.0–8.0) conditions (data not shown). The mutant showed no increase in autolysis (Figure S2A), and killing of the ΔGacI mutant by lysozyme or the cell wall-active antibiotics vancomycin and nafcillin was even slightly slower than observed with the parent strain (Figures S2B–S2D). Also, in contrast to tunicamycin-treated GAS that completely lack GAC expression, the ΔGacI mutant is not more sensitive to mutanolysin (Figure S2E) nor defective in peptidoglycan formation as measured by vancomycin-BODIPY labeling (Figure S2F).

Phenotypic Characterization of ΔGacI Expressing GlcNAc-Deficient GAC

The isogenic ΔGacI mutant was compared to the WT GAS M1T1 parent strain to examine the phenotypic and functional consequences of loss of the GlcNAc side chain from the GAC. The mutant and parent strains grew equally well in bacteriologic media (Figure 4A) and did not differ with respect to well-known virulence factors or traits including surface-anchored M1 protein expression, hyaluronic acid capsule production, fibrinogen

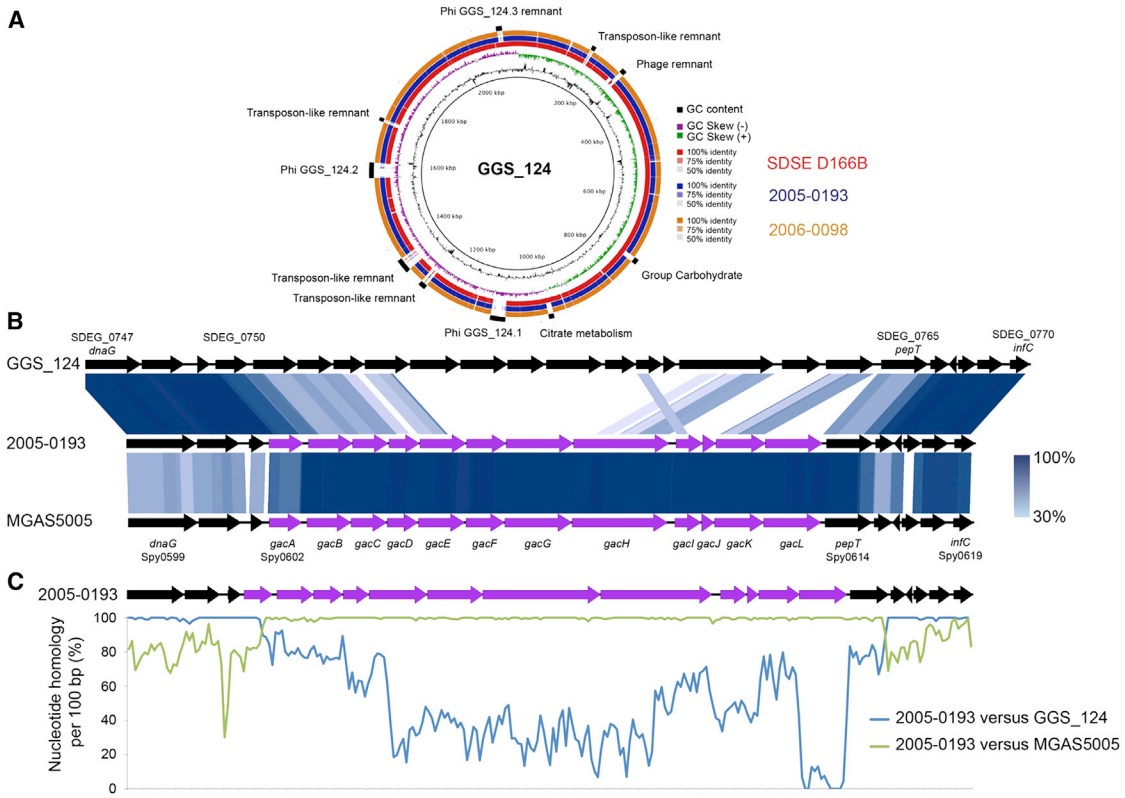

Figure 2. *Streptococcus dysgalactiae* subsp. *equisimilis* Testing Positive for GAC Possess the *gacA–gacK* Gene Locus

(A) Circular genome map of the group G carbohydrate expressing *Streptococcus dysgalactiae* subsp. *equisimilis* (SDSE) GGS_124 genome (accession number AP010935) with BLAST comparisons to the completely sequenced group G carbohydrate expressing SDSE strain SDSE_D166B genome (accession number CP002215) and the draft genomes of two SDSE strains expressing the GAC antigen, 2005-0193 and 2006-0098. The comparative map was created using BRIG. The innermost rings show GC content (black) and GC skew (purple/green) of GGS_124. The three outer rings show BLAST comparisons (using BLASTn and an E-value cutoff of 10.0) to SDSE_D166B (red) and to the draft genome sequences of 2005-0193 (blue) and 2006-0098 (orange). The legend shows the percent identity of BLASTn hits to the GGS_124 reference. Both genomes share similar genome synteny with both GGS_124 and SDSE_D166B. Labels around the outer ring refer to genomic regions present in GGS_124 but not in the two SDSE strains expressing GAC, including the GAC carbohydrate gene cluster.

(B) Genome architecture of the carbohydrate loci located between the *dnaG* to *infC* gene sequences from 2005-0193 with GGS_124 and M1 strain MGAS5005. Regions of genetic similarity were determined using BLAST with graphical representation of syntenic gene content designated using EasyFigure 2.1. Purple coding sequences refer to the GAC-encoded *gacA–gacL* cluster. Blue shaded regions between the stacked genome sequences reflect conserved gene content with percent homology indicated by the legend.

(C) Similarity plot showing carbohydrate locus nucleotide sequence conservation between 2005-0193 versus GGS_124 (blue line) and 2005-0193 versus MGAS5005 (green line). Evidence of homologous recombination between a GAS donor and the SDSE progenitor is evident between the *gacA* and *pepT* genes. The plot was generated from a Clustal alignment of sequence between the *dnaG* and *infC* using a sliding window of 100 bp with values plotted as an average over a 100 bp sliding window.

binding, cysteine protease (SpeB) activity, surface plasmin acquisition due to streptokinase, or sugar metabolism (Figures 4B–4G). Analysis of total protein preparations by gel electrophoresis and silver stain showed a similar pattern for WT and ΔGacI mutant (Figure S3A). Interestingly, the ΔGacI mutant produced longer chains in stationary phase cultures (average 16.6 cocci) than the parent strain (average 6.7 cocci) (Figure S3B). Differences in average chain lengths were less pronounced in exponential phase cultures: WT = 11.2 cocci versus ΔGacI = 15.6 cocci. While the elongated chains indicate a fundamental problem in cell division or chaining, transmission electron microscopy of WT and ΔGacI revealed no apparent differences in the ultrastructural appearance of the bacterial cell walls (Figure S3C), findings consistent with a previous report on "A-variant" strains isolated from mice (Swanson and Gotschlich, 1973).

The GlcNAc Side Chain of GAC Promotes GAS Survival in the Presence of Whole Blood, Serum, Neutrophils, and Antimicrobial Peptides

Since GAC is localized at the host-pathogen interface, we next assessed survival of the ΔGacI mutant in assays modeling critical steps in invasive disease pathogenesis. Compared to the WT and GacI* complemented strains, the ΔGacI mutant was attenuated in whole-blood survival (Figures 5A and 5B) and resistance to killing by isolated human neutrophils (Figure 5C), despite similar phagocytic uptake (Figures S4A–S4C). Accelerated killing of the ΔGacI mutant persisted in the presence of cytochalasin D (Figures 5B and 5C), an actin microfilament inhibitor that impairs phagocytosis. Thus, it appeared that the ΔGacI mutant was sensitized to extracellular neutrophil killing, which predominantly occurs through DNA-based neutrophil

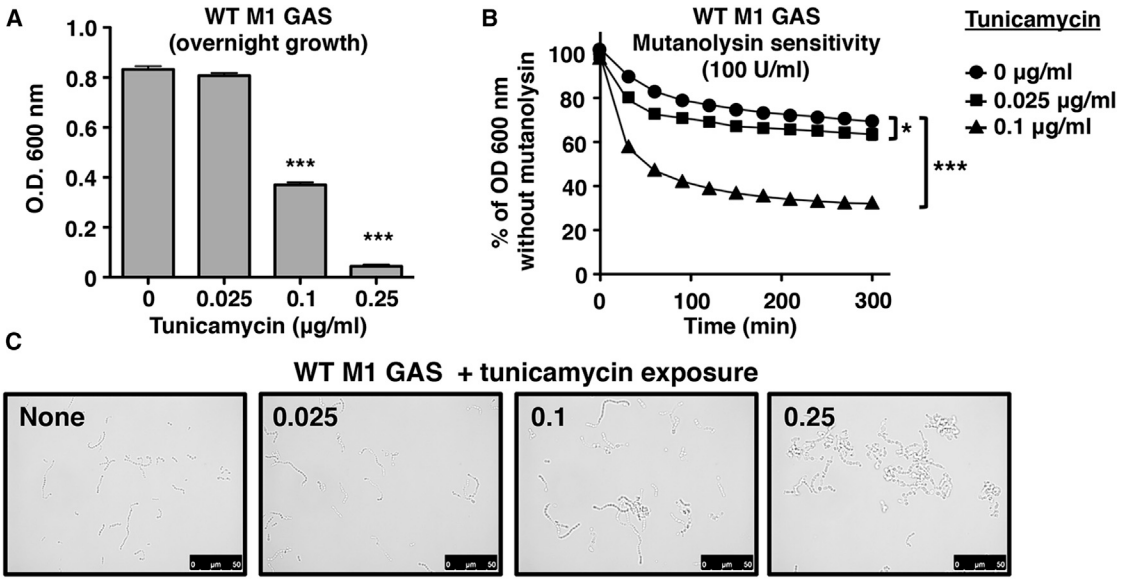

D

Composition Analysis

	Rha	Man	Glc	GlcNAc	PS (μg)
Wild-Type M1 GAS	57.49	0.44	1.06	41.01	417.5
WT + 0.025 Tun	0	100	0	0	0.027
WT + 0.1 Tun	0	0	0	0	0

Figure 3. TarO/GbcO Homolog M5005_Spy0240 Contributes to GAC Biosynthesis

(A and B) Tunicamycin is a specific inhibitor of UDP-GlcNAC:lipid phosphate transferases like TarO and GbcO and produces a similar phenotype to a *gbcO* knockout in group B *Streptococcus* (GBS). WT M1 GAS was treated with different concentrations of tunicamycin to inhibit the activity of homologous enzyme encoded by the *gacO* gene (M5005_Spy0240), which resulted in (A) growth inhibition (mean ± SEM of four independent experiments, one-way ANOVA) and (B) increased sensitivity to mutanolysin (100 U/ml; mean ± SEM of two independent experiments, two-way ANOVA); *$p < 0.05$, **$p < 0.01$, ***$p < 0.001$.

(C and D) Changes in cell morphology (C) and complete loss of rhamnose expression indicating a loss of GAC production (D). Abbreviations: Rha, rhamnose; Man, mannose; Glc, glucose; GlcNAc, *N*-acetyl-glucosamine; PS, polysaccharide; Tun, tunicamycin at indicated concentration (μg/ml). See also Figure S2.

extracellular traps (NETs) (Brinkmann et al., 2004) and potentially other antimicrobial components in human blood. Correspondingly, WT GAS and ΔGacI mutant strains were equally susceptible to hydrogen peroxide and superoxide (Figures S4D and S4E). Exposure of neutrophils to WT GAS and ΔGacI mutant strains induced formation of NETs equally (Figure S4F); however, the mutant was more susceptible to killing within NETs (Figure 5D) and to the human cathelicidin antimicrobial peptide LL-37 (Figure 5E and Figure S4G). LL-37 is a component of neutrophil-specific granules important for intracellular killing and is deployed within NETs. To examine the specific contribution of GAC and its GlcNAc side chain in modulating LL-37 affinity for GAS, we purified WT and mutant GAC and used surface plasmon resonance to measure its interaction with the host defense peptide. Both WT and ΔGacI mutant GAC bound to immobilized LL-37; however, the binding of the ΔGacI mutant GAC to the host defense peptide was substantially stronger than WT GAC at all polysaccharide concentrations tested (Figure 5F). The calculated Kd values obtained by kinetic measurements using a 1:1 Langmuir fitting model were 130 μM for the WT GAC and 44 μM for the ΔGacI mutant GAC. This finding shows that the GlcNAc side chain of GAC itself markedly influences LL-37 affinity for its cell wall target. Increased cell surface hydrophobicity, as measured by *n*-hexadecane partition of the intact bacterium, suggested a potential basis for increased LL-37 binding and sensitivity (Clarke et al., 2007) of the ΔGacI mutant (Figure 5G).

Serum, but not plasma, possesses high levels of bactericidal activity against Gram-positive bacteria due to the presence of platelet-derived antimicrobials that are released during the clotting process (Hirsch, 1960). We initially examined baby rabbit serum (BRS), which lacks preexisting anti-GAS antibodies. The GAS ΔGacI mutant was sensitive to killing in BRS, a difference that persisted upon heat inactivation of complement activity (Figure 5H). Similarly, the ΔGacI mutant had reduced growth in human serum (Figure 5I), but WT and mutant strains survived equally well in human plasma (Figure 5J) and accumulated similar levels of surface C3b (Figure 5K). Serum but not plasma sensitivity suggested a role for platelets, important in host defense against GAS (Hirsch, 1960; Yeaman, 2010). As inferred, the ΔGacI mutant was found to be hypersensitive to killing by the releasate of thrombin-activated washed human platelets (Figure 5I).

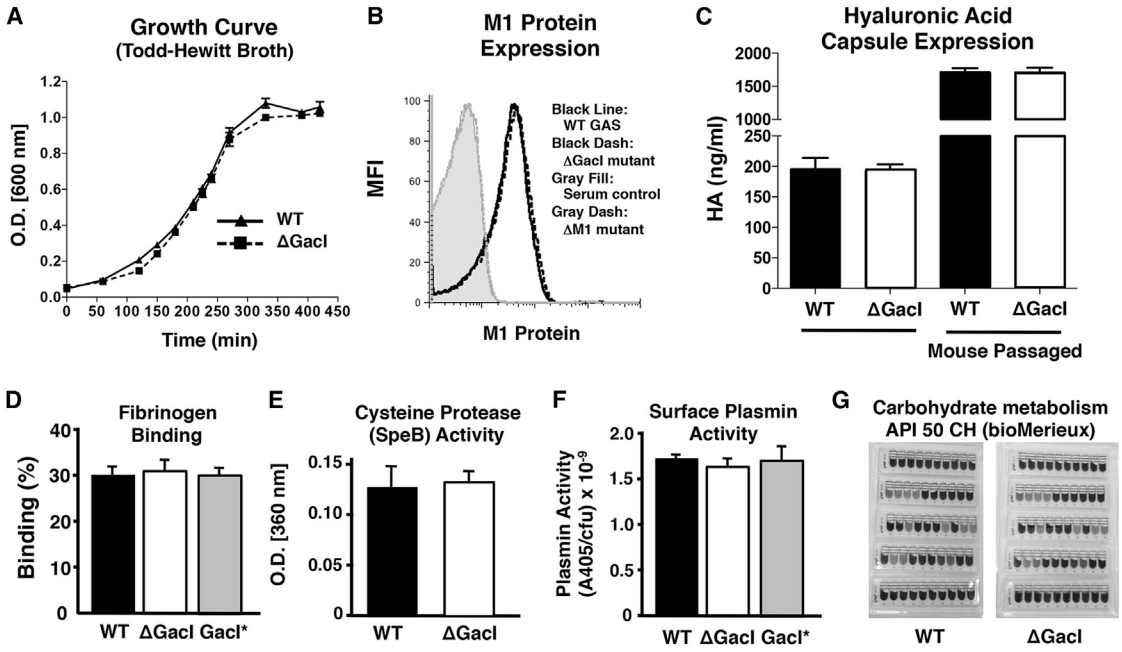

Figure 4. ΔGacI Mutant Bacteria Are Not Impaired in Expression of Several Known GAS Virulence Factors or Traits

(A–F) GAS WT and ΔGacI mutant bacteria were assessed for (A) growth in Todd-Hewitt broth (mean ± SD of a representative experiment); (B) M1 protein expression (gray fill, serum control; black line, WT GAS; black dash, ΔGacI; gray dotted, GacI* reconstituted); (C) capsule expression in lab-grown and animal-passaged bacteria (mean ± SEM of two independent experiments); (D) fibrinogen binding; (E) SpeB secretion; (F) plasmin accumulation of GAS WT, ΔGacI mutant, and GacI*. Pooled normalized data from three independent experiments are shown (mean ± SEM; one-way ANOVA).

(G) Carbohydrate metabolism of GAS WT and ΔGacI mutant assessed using diagnostic API 50 CH test (BioMerieux; t = 48 hr). Yellow color indicates the specific carbohydrate is fermented, whereas blue/purple color indicates the bacteria do not metabolize the sugar. See also Figure S3.

The GAC GlcNAc Side Chain Is Required for Full GAS Virulence In Vivo

Given the increased susceptibility of the ΔGacI mutant to whole-blood, neutrophil, cathelicidin, and serum (platelet-derived antimicrobial) killing, we examined whether loss of the GlcNAc side chain affected GAS pathogenicity in vivo. In a rabbit model of pulmonary infection, no mortality was seen following challenge with the ΔGacI mutant at a dose where the WT strain caused 89% mortality (Figure 6A). Gross and microscopic examination of the lungs of WT GAS-infected rabbits revealed extensive hemorrhagic necrosis amid diffuse bacterial and leukocytic infiltrates, changes that were markedly reduced in the lungs of surviving ΔGacI-infected animals (Figure 6B and Figure S5A). Assessed early in infection (12 hr), WT GAS infection was associated with higher fever (Figure 6C), greater bacterial load in the lung (Figure 6D), and increased lung TNF-α levels (Figure 6E) compared to ΔGacI mutant-infected rabbits. Likewise, the ΔGacI mutant produced significantly lower mortality in a mouse systemic infection model (Figure 6F), in association with lower bacterial counts in blood (Figure 6G) and serum TNF-α levels (Figure S5B). Thus, the GlcNAc side chain of the GAC is a virulence determinant increasing bacterial survival and resistance to host immune clearance in vivo.

The GAC Polyrhamnose Backbone Is a Vaccine Antigen Candidate

There is a lack of consensus regarding the role of the GAC GlcNAc side chain in the immunopathogenesis of rheumatic fever. Using the GlcNAc-deficient GAC extracted from ΔGacI mutant bacteria as a tool, we assessed recognition of this altered antigen by an autoreactive human monoclonal antibody (3B.6) derived from a patient with rheumatic carditis that binds to heart valve and myocardium, to GAS bacteria, and to GlcNAc-albumin, but not to albumin alone (Galvin et al., 2000). 3B.6 showed markedly reduced binding to the ΔGacI mutant carbohydrate compared to the native GAC (Figure 7A), lending support to the hypothesized role of GAC GlcNAc in the pathogenesis of rheumatic carditis. We considered whether the GlcNAc-deficient GAC (ΔGAC), as purified from the ΔGacI mutant, could elicit an antibody response that facilitates opsonization and immune killing of diverse GAS serotypes. A conjugate vaccine antigen complex, consisting of a protein + GlcNAc-deficient GAC, was prepared using affinity interactions (Zhang et al., 2013) and then used to raise a polyclonal rabbit anti-ΔGAC antiserum. The final antiserum was highly reactive against the immunizing antigen, ΔGacI mutant GAC (1:307,200, control nonimmune serum 1:1,200), as well as the native GAC (1:307,200, control nonimmune serum 1:1,200), indicating that recognition was not shielded by presence of GlcNAc. Anti-ΔGAC IgG efficiently bound to intact WT M1 GAS bacteria as well as GAS strains representing seven additional common disease-associated serotypes (Figure 7B) and promoted bacterial killing by human whole blood (M1) and neutrophils (M1 + 8 additional GAS serotypes) (Figures 7C and 7D). Finally, as proof-of-concept, administration of the anti-ΔGAC antiserum provided passive protection in a

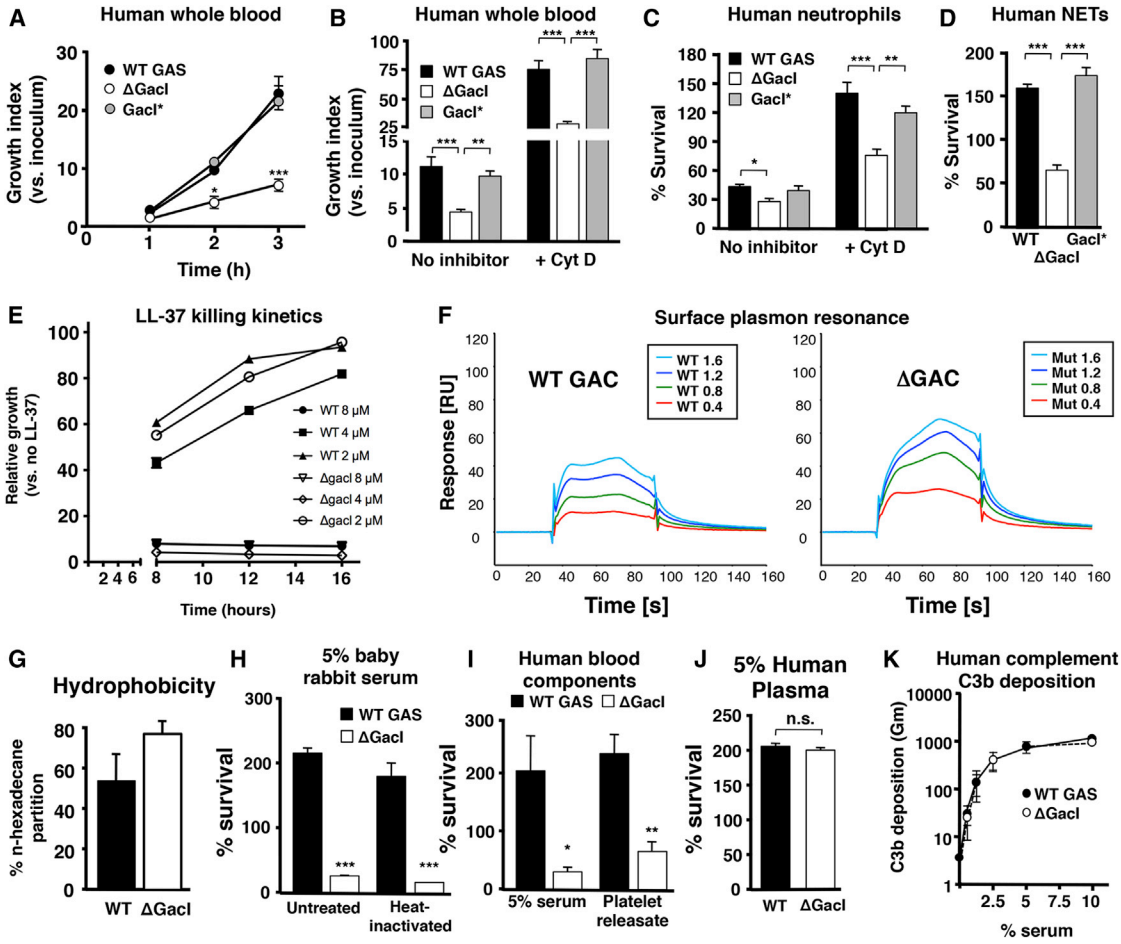

Figure 5. Antigen-Negative GAS Display Increased Sensitivity to Neutrophil and Platelet Immune Defenses

(A and B) ΔGacI mutant bacteria are defective in whole-blood proliferation both in the absence (A) and presence (B, +cytochalasin D, CytD, 25 μg/ml) of phagocytosis. Data in (B) represent the 2 hr time point. Pooled data from three independent experiments are shown (mean ± SEM; one-way ANOVA).

(C) Total (no inhibitor) and extracellular (+Cyt D, 10 μg/ml) bacterial killing by isolated human neutrophils. Surviving cfu were quantified after 15 min and 30 min for total killing and extracellular killing, respectively. Combined data from three independent experiments using different donors are shown (mean ± SEM; one-way ANOVA).

(D) Survival of bacteria in neutrophil extracellular traps (NETs). Neutrophils were incubated with 25 nM PMA for 3 hr and incubated with bacteria for 30 min. Pooled data from two independent experiments are shown (mean ± SEM, one-way ANOVA).

(E) Kinetic analysis showing increased susceptibility to cathelidicin antimicrobial peptide LL-37 for the ΔGacI mutant compared to WT.

(F) Surface plasmon resonance (SPR) analysis. LL-37 peptide was immobilized on a CM5 sensor chip by amine coupling. Various concentrations of purified WT (left) or ΔGacI mutant GAC (right) were used as analytes to detect binding to LL-37. SPR sensorgrams were generated by subtraction of the reference flow cell and the signals obtained by injection of only the running buffer from the measured response units.

(G) Increased hydrophobicity of the ΔGacI mutant bacteria compared to GAS WT as assessed by the n-hexadecane partition assay. The y axis indicates the percent of original inoculum recovered from the n-hexadecane layer.

(H) Survival of GAS WT or ΔGacI mutant strain in 5% complement-sufficient or heat-inactivated (HI) baby rabbit serum (BRS). Survival was quantified after 5 hr incubation at 37°C. Representative data are shown.

(I) Effects of human serum or thrombin-activated platelet supernatant on survival of GAS WT or ΔGacI mutant bacteria. Serum and platelets were collected from the same donor, processed as described in the Experimental Procedures, and added to a final concentration of 5% and 25%, respectively. Pooled data from five independent experiments are shown (mean ± SEM; ratio t test). *$p < 0.05$, **$p < 0.01$, ***$p < 0.001$.

(J) No difference in growth of GAS WT or ΔGacI mutant strain in 5% human plasma (mean ± SEM, t test).

(K) C3b deposition on GAS WT and ΔGacI bacteria after incubation with a range of serum concentrations. Pooled data from four independent experiments are shown (mean ± SEM). See also Figure S4.

murine systemic infection model with a heterologous (GAS M49) strain (Figure 7E). Efficacy of the anti-ΔGAC antiserum in promoting neutrophil opsonophagocytosis and passive immune protection compared favorably to an antiserum reactive against the WT GAC prepared through an identical procedure (Figures S6A–S6C). Neither rabbit postimmune antiserum demonstrated cross-reactivity to human cardiac antigens (Figures S6D and S6E), consistent with findings reported in postimmune mouse antisera against a WT GAC conjugate antigen (Sabharwal et al., 2006).

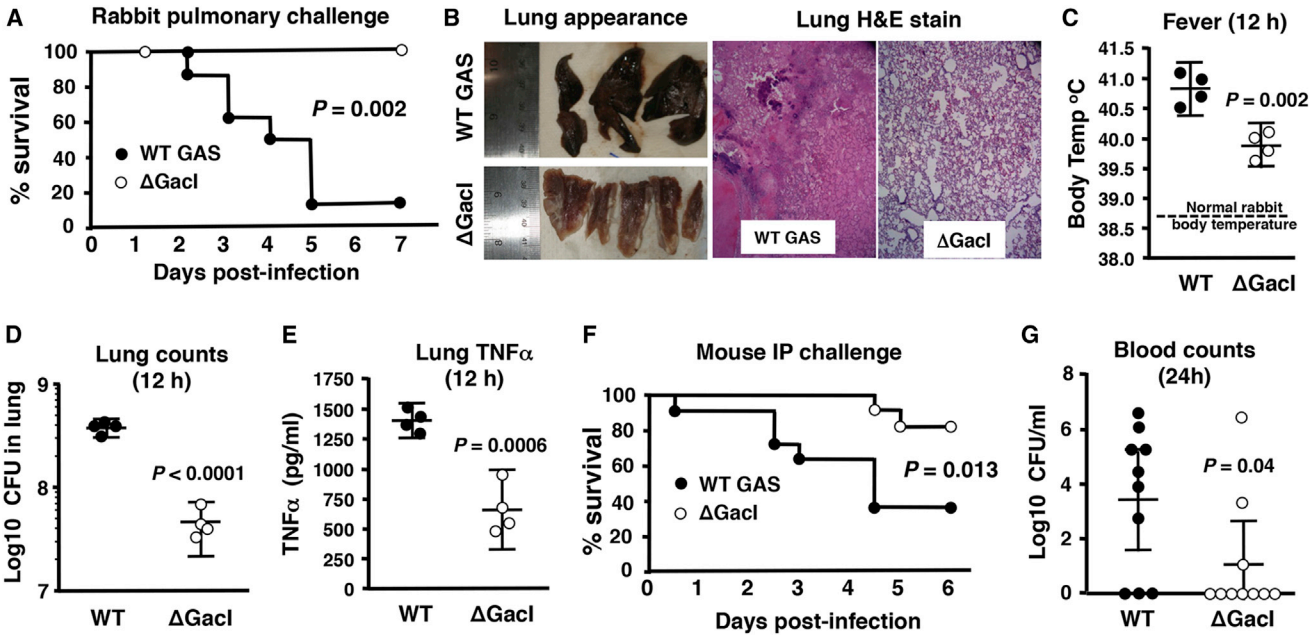

Figure 6. Loss of the GAC GlcNAc Side Chain Attenuates GAS Virulence

(A) Survival curve of rabbits infected with GAS WT or ΔGacI mutant bacteria. Rabbits were infected with 4×10^9 cfu intrabronchially, and survival was monitored for 7 days (n = 9 rabbits of either sex per group in three independent experiments; log rank test).

(B) Gross lung appearance and microscopic H&E stain of rabbit lungs after infection with GAS WT or ΔGacI mutant bacteria.

(C–E) Body temperature (C), lung bacterial counts (D), and lung TNF-α levels (E) in lungs of infected rabbits 12 hr after intrapulmonary challenge; n = 4 rabbits per group; t test; mean and 95% confidence interval.

(F) Survival curve of mice upon systemic infection with GAS WT or ΔGacI mutant bacteria; survival was monitored for 6 days (n = 11 per group; log rank test).

(G) Blood cfu of mice 24 hr post-systemic infection (n = 10 mice per group; t test; mean and 95% confidence interval). *p < 0.05, ***p < 0.001. See also Figure S5.

DISCUSSION

We have studied aspects of the biology of the hallmark GAC cell wall antigen of GAS through the identification and subsequent mutation of the genetic locus encoding its biosynthesis. An isogenic mutant GAS strain lacking the species-defining GlcNAc side chain had markedly reduced survival in human blood and systemic animal infection models, with increased sensitivity to neutrophil and serum killing identified as key elements underlying the virulence attenuation. Although phagocytic uptake, complement deposition, and killing of WT GAS and ΔGacI mutant were similar, the mutant was hypersusceptible to human cathelicidin LL-37 and the antimicrobial action of factors released by thrombin-activated platelets. Loss of the GlcNAc side chain on GAC did not produce a general defect in GAS cell wall integrity, as the ΔGacI mutant did not differ from WT in susceptibility to autolysis, reactive oxygen species, lysozyme, nafcillin, or vancomycin. GAS growth in bacteriologic media, tissue culture media, and plasma were unaffected by loss of the GlcNAc side chain, but the average chain length of the mutant strains was increased. Although several well-characterized GAS virulence factors were unaltered (e.g., M1 protein, capsule, cysteine protease, surface plasmin acquisition), future studies may reveal additional mechanisms by which the GlcNAc side chain interacts with other bacterial surface components to influence the host-pathogen interaction. Elimination of a key structural feature of the most abundant GAS cell wall component no doubt changes the full context in which other GAS cell wall-associated molecules are displayed and potentially modulates their access to soluble factors, matrix components, or cellular receptors present in host tissues. Our studies were performed in an invasive GAS isolate representative of the globally disseminated serotype M1T1 clone, and the relative contribution of the GlcNAc side chain to virulence might vary dependent on the quorum of other innate immune resistance factors present in a given GAS serotype.

A variety of published clinical data, summarized in the introduction, has raised concern about the potential of the GAC GlcNAc side chain to provoke cross-reactive antibodies relevant to the immunopathogenesis of rheumatic fever. While anti-GlcNAc antibodies correlate with the presence and severity of rheumatic heart disease (Ayoub et al., 1974; Dudding and Ayoub, 1968; Shulman et al., 1974; Appleton et al., 1985), and anti-GlcNAc monoclonal antibodies cross-reactive for heart or brain tissue have been derived from patients with rheumatic fever (Galvin et al., 2000; Kirvan et al., 2003), these clinical associations have proven difficult to corroborate experimentally, since there is no faithful animal model of rheumatic fever, and cardiac cross-reactive antibodies are not readily elicited in experimental immunization of mice (Sabharwal et al., 2006) or rabbits (this study).

In 2004, the U.S. National Institute of Allergy and Infectious Diseases convened an expert workshop of scientists, clinicians, government agencies, and the pharmaceutical industry to review the available data and to explore the microbiologic, immunologic, epidemiologic, and economic issues involved in development and implementation of a safe and effective GAS vaccine,

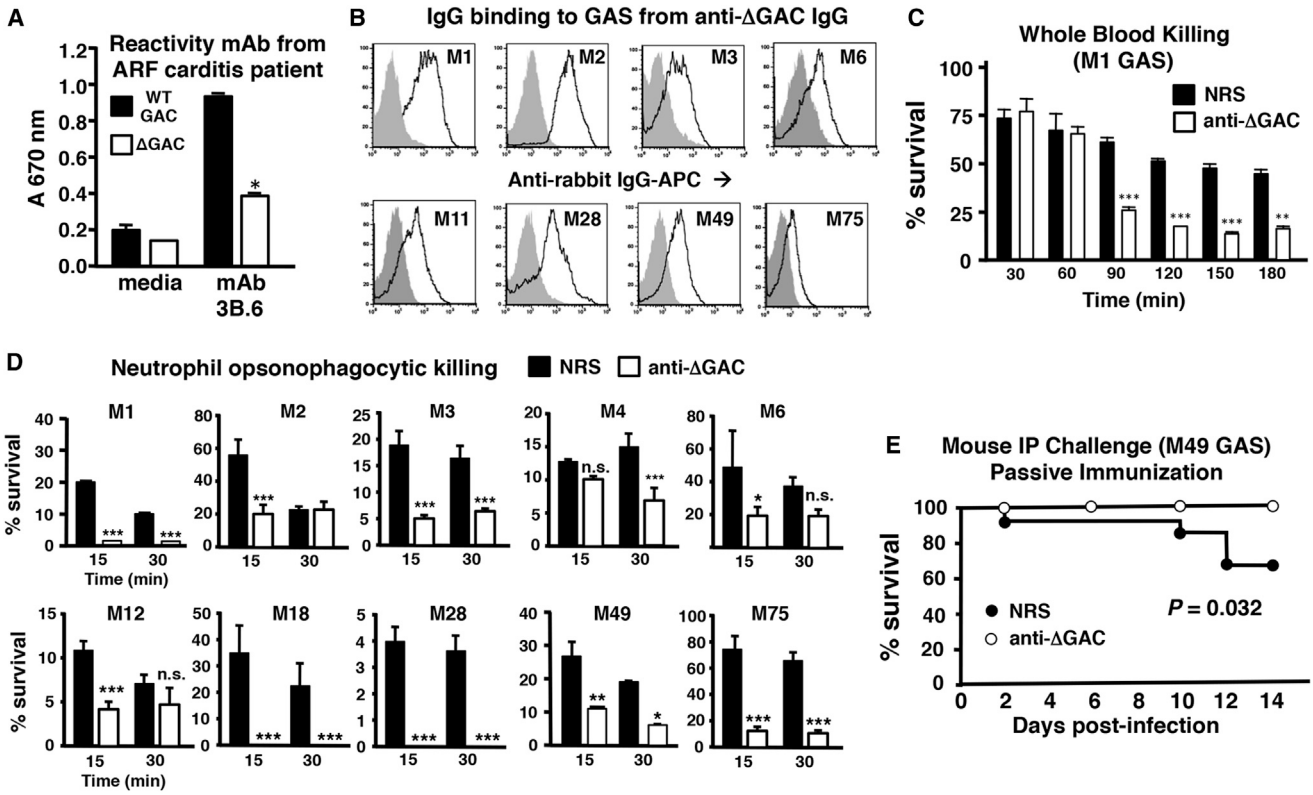

Figure 7. Antiserum Raised against GlcNAc-Deficient GAC Promotes Opsonophagocytosis of Multiple GAS Serotypes

(A) GlcNAc-specific human monoclonal antibody (mAb) 3B6 derived from a patient with rheumatic carditis (Galvin et al., 2000) shows significantly reduced cross-reactivity with GlcNAc-deficient GAC. *$p < 0.05$ (t test; mean ± SEM).

(B) Binding of polyclonal anti-ΔGAC IgG (black line) to WT GAS of eight different disease-associated serotypes; gray fill, nonimmune rabbit IgG control. Serotype is indicated in histogram.

(C) Enhanced killing of WT M1 GAS in human whole blood upon addition of anti-ΔGAC rabbit antiserum versus normal rabbit serum (NRS). Mean ± SD of a representative experiment.

(D) Improved opsonophagocytic killing of multiple GAS serotypes by isolated human neutrophils upon addition of anti-ΔGAC antiserum versus NRS; mean ± SEM, t test. *$p < 0.05$, **$p < 0.01$, ***$p < 0.001$; n.s., not significant.

(E) Mice are protected from infection with WT GAS M49 through passive immunization with ΔGAC antiserum versus NRS (n = 12 per group; log rank test). See also Figure S6.

a sentinel event toward the lifting of the 30 year Food and Drug Administration ban on GAS vaccine research set in place because of the suspected development of rheumatic fever in vaccine subjects in early trials. The report summarizing the deliberations of the workshop (Bisno et al., 2005) stated:

> Molecular mimicry—sharing of antigenic determinants between the host and antigens of GAS—has been implicated in ARF and rheumatic heart disease and has represented a major obstacle for vaccine development. GAS antigens, including the M proteins and group A carbohydrate, have been shown to contain epitopes that mediate B and/or T cell cross-reactions with human tissue antigens. Because the precise role of molecular mimicry in the pathogenesis of ARF has not been established, every effort should be made to exclude tissue-cross-reactive epitopes during vaccine development.

Our proof-of-principle demonstration that antisera raised against the polyrhamnose core of GAC, as purified from the ΔGacI mutant, may still provide significant broad-spectrum opsonophagocytic activity is at minimum consistent with this encouragement.

In summary, we have demonstrated that the classical Lancefield antigen is not simply a structural component of the GAS cell wall but rather an important virulence determinant. In addition, the side chain-deficient core backbone of the GAC, containing only the nonmammalian polyrhamnose structure and lacking the potentially autoimmune GlcNAc epitope, merits future exploration as a component of universal GAS vaccines.

EXPERIMENTAL PROCEDURES

Bacterial Strains and Genetic Manipulations

Principal strains analyzed were GAS M1T1 5448 (Kansal et al., 2000) and M49 NZ131 (Simon and Ferretti, 1991), and *Streptococcus dysgalactiae* subsp. *equisimilis* (SDSE) strains (2005-0193 and 2006-0098) reactive for GAC (McMillan et al., 2010). Other GAS serotype strains were obtained from the CDC Streptococcal Laboratory (B. Beall, Director). Insertional mutation of *gacD* through *gacH, and gacJ* through *gacL* was performed as described (Hollands et al., 2010) with osmotic protection in THB 0.5 M sucrose. Precise

in-frame allelic replacement of the *gacI* gene was performed using established methodology (Pritzlaff et al., 2001). Genetic complementation of ΔGacI with the *gacI* gene on multicopy plasmid vector pDCerm resulted in incomplete complementation, suggesting perturbation of gene regulatory networks or improper stoichiometry of the enzymes involved GAC biosynthesis. Therefore, we performed genomic complementation with a "watermarked" copy of *gacI* to allow discrimination from authentic WT cultures. Details of these techniques are provided in the Supplemental Information.

Whole-Blood Proliferation and Phagocytosis Assay

Bacteria were incubated with lepirudin anticoagulated blood from healthy donors in siliconized tubes at 37°C. For vaccine-related assays, rabbit anti-WT GAC serum, anti-ΔGAC serum, or nonimmune normal rabbit serum diluted 1:5 in PBS was added. Surviving colony-forming units (cfu) were quantified by dilution plating. Cytochalasin D (25 μg/ml) was used to block phagocytosis. Whole-blood phagocytosis was performed under shaking conditions with FITC-labeled bacteria and analyzed by flow cytometry.

Lectin Staining, M1 Protein Expression, and IgG Binding

Overnight cultures were centrifuged and resuspended in HEPES++ buffer (20 mM HEPES, 140 mM NaCl, 5 mM $CaCl_2$, 2.5 mM $MgCl_2$ [pH 7.4]) + 0.1% bovine serum albumin (BSA) (HEPES++ 0.1% BSA) to OD_{600} = 0.4. The bacterial suspension (100 μl) was pelleted and stained with FITC-labeled succinylated wheat germ agglutinin (sWGA) to assess GlcNAc expression. M1 protein expression was quantified on bacterial cultures at an OD_{600} = 0.6 using anti-M1 or sham mouse serum and PE-conjugated anti-mouse IgG. To test IgG binding, bacterial cultures were grown to OD_{600} of 0.4, washed, resuspended in buffer, and preincubated with 10% heat-inactivated normal horse serum to block Fc-binding proteins. After washing, samples were incubated with 0.1 mg/ml control rabbit IgG (Jackson Immunoresearch) or purified anti-ΔGAC rabbit IgG followed by allophycocyanin-conjugated goat anti-rabbit IgG. Staining was analyzed by flow cytometry.

Neutrophil Experiments

Human neutrophils were isolated from healthy donor blood using the Polymorphprep system (Axis-Shield). Neutrophils were seeded into 96-well flat-bottom tissue culture-treated plates (Costar) in RPMI 1640 (Invitrogen) + 2% fetal bovine serum (FBS) heat-inactivated at 70°C. Bacteria were added at a multiplicity of infection (moi) of 0.1; plates were centrifuged and incubated at 37°C with 5% CO_2 for 30 min. Neutrophils were lysed and bacterial survival (versus control wells lacking neutrophils) was determined by dilution plating. Extracellular neutrophil killing was assessed by pretreating neutrophils with cytochalasin D (10 μg/ml). For opsonophagocytic assays, exponential phase bacteria were preincubated with anti-WT GAC rabbit serum, anti-ΔGAC rabbit serum, or NRS diluted 1:5 in PBS and added to neutrophils at a moi of 0.1. NET quantification was determined by counting extracellular traps after staining with Sytox Orange. NET killing assays were performed as above with preincubation of neutrophils in 25 nM phorbol 12-myristate 13-acetate (PMA) for 3 hr to maximally induce NETs (Akong-Moore et al., 2012).

LL-37 Susceptibility

LL-37 minimum inhibitory concentrations (MICs) were determined by incubating log phase cultures in DMEM 10% THB with different concentrations of LL-37 for 24 hr at 37°C. For kinetic analysis, GAS WT and ΔGacI mutant bacteria were grown and resuspended as for MIC assays and incubated with different concentrations of LL-37, and growth was recorded by measuring OD_{600} every 30 min for 20 hr using the Bioscreen C MBR machine.

Serum, Plasma, and Platelet Survival Assays

Serum and/or plasma (lepirudin) were collected from healthy individuals and used immediately or stored at −80°C. Bacterial survival in 5% serum, plasma, or 25% platelet releasate was performed as described (Rooijakkers et al., 2010). Survival/growth was calculated as the ratio of bacteria cfu surviving after incubation compared to the initial inoculum.

GAC Purification and Carbohydrate Analysis

Cell pellets of bacterial strains were resuspended in cold 48% aqueous hydrogen fluoride (HF), sonicated, and stirred at 4°C for 48 hr. Next, ice-cold H_2O was added to each bacterial suspension and the material was dialyzed against cold H_2O. Dialyzed preparations were centrifuged to remove cellular debris, and supernatant containing polysaccharide was lyophilized. Finally, polysaccharide (HF-PS) was purified by size-exclusion chromatography, and positive fractions were pooled and lyophilized. Monosaccharide composition analysis was performed using gas chromatography/mass spectrometry as alditol acetate (AA) derivatives. Linkage analysis was performed on partially methylated alditol acetate (PMAA) derivatives.

In Vivo Virulence

For the pulmonary infection model, rabbits (total n = 13 over four independent experiments, either sex; eight male, five female) were infected with 4×10^9 cfu of GAS WT or ΔGacI mutant bacteria intrabronchially, and survival was monitored for 7 days (n = 9 rabbits). Lungs from a fourth cohort were harvested after 12 hr (n = 4 rabbits; two male, two female) and homogenized for cfu counts and TNF-α levels (ELISA, R&D Systems). For the mouse systemic infection model, log phase bacteria were resuspended in PBS 5% porcine gastric mucin. Female 10-week-old CD-1 mice were injected intraperitoneally (i.p.) with 2×10^6 cfu/200 μl GAS WT or ΔGacI mutant bacteria. Survival was monitored twice daily for 6 days. A second group of ten CD-1 female mice was similarly injected with GAS WT or ΔGacI and blood; serum and organs were harvested at 24 hr and homogenized for bacterial cfu counts.

Preparation of WT and ΔGAC Protein Conjugates and Rabbit Polyclonal Antisera

GAC purified from WT GAS (WT GAC) and the ΔGacI mutant (ΔGAC) were coupled to recombinant pneumococcal protein SP_0435 using streptavidin-biotin affinity interactions, and the complexes were purified by gel filtration chromatography to > 95% purity (Zhang et al., 2013). Polyclonal rabbit antibodies were raised against MAPS-conjugated WT GAC and ΔGAC through Cocalico Biologicals; see Supplemental Information for details.

Mouse Passive Immunization and Challenge

Cohorts of female 10-week-old CD-1 mice (Charles River Labs) were immunized i.p. with 0.5 ml anti-ΔGAC rabbit serum (n = 12) or normal rabbit serum (NRS; MP Biomedicals) (n = 12) diluted 1:5 in PBS 3 hr prior to infection with serotype M49 GAS strain NZ131. Log phase bacteria were resuspended in PBS plus 5% porcine gastric mucin. Mice were challenged i.p. with WT M49 GAS (2.5×10^7 cfu/200 μl) and survival was monitored twice daily for 10 days.

Ethics Statements

Human blood and neutrophils were collected after informed consent from healthy human volunteers as approved by the University of California San Diego (UCSD) Human Research Protection Program. Animal infection studies were carried out in strict accordance with the recommendations in the Guide for the Care and Use of Laboratory Animals of the National Institutes of Health. Protocols were approved by the Institutional Animal Care and Use Committees (IACUC) at the University of Minnesota (rabbits), University of Iowa (rabbits), and UCSD (mice). All efforts were made to minimize the suffering of animals employed in this study.

Statistical Analysis

All statistical analyses were performed using GraphPad Prism version 5.0d (GraphPad Software Inc.) and display experimental data of at least two independent experiments performed in triplicate, displaying mean and standard error of mean (SEM) throughout the manuscript, except for animal-related experiments, which display mean ± 95% confidence intervals. The following statistical tests were applied: comparisons between three or more groups, one-way ANOVA; comparison between two groups, Student's t test; time course experiments, two-way ANOVA; animal survival curves, log rank test. Statistical significance was accepted at $p < 0.05$. *$p < 0.05$, **$p < 0.01$, ***$p < 0.001$.

SUPPLEMENTAL INFORMATION

Supplemental Information includes Supplemental Experimental Procedures and six figures and can be found with this article online at http://dx.doi.org/10.1016/j.chom.2014.05.009.

AUTHOR CONTRIBUTIONS

N.M.v.S., J.N.C., K.K., A.H., A.K.-F., L.L., E.T.M.B., F.Z., S.D, L.S., J.G., J.H., B.L., S.H.M.R., R.M., S.J.S., P.M.S., and V.N. participated in designing the experiments. N.M.v.S., J.N.C., K.K., S.D., L.L., L.S., and J.G. performed genetic manipulation of GAS and in vitro and in vivo assays. R.K.A. performed bioinformatics analysis of the GAC locus. G.D., M.R.D., and M.J.W. collected, sequenced, and analyzed genome sequence data from hybrid GGAS strains. F.Z. and R.M. designed and constructed protein-polysaccharide complexes of mutant and WT GAC to raise rabbit antisera. M.C. provided monoclonal antibody from carditis patients and performed immunohistochemical analyses. P.M.S. and J.A.M. designed and performed rabbit infection experiments. E.T.M.B. and S.H.M.R. designed and performed whole-blood phagocytosis and complement assays. A.K.-F. and S.J.S. designed and participated in platelet experiments. J.H. and B.L. performed the surface plasmon resonance studies with LL-37 and purified native and mutant GAC. B.C. performed all the glycoanalysis. N.M.v.S. and V.N. wrote the manuscript and other authors provided comments.

ACKNOWLEDGMENTS

This research was supported by NIH/NIAID grants to V.N., NHLBI-supported UCSD Program in Excellence in Glycosciences (V.N., B.C.), a Marie Curie International Incoming Fellowship and NIH T32 Training Grant to N.M.v.S., a CJ Martin Overseas Postdoctoral Training Fellowship (514639) and Project Grant APP1033258 to J.N.C. from the Australian National Health and Medical Research Council, the NIAID-supported Great Lakes Regional Center for Excellence in Biodefense and Emerging Diseases (AI57153) where P.M.S. and V.N. are members, NIH grants HL35380 and HL5627 to M.W.C., and Collaborative Research Center (SFB) 765 to J.H. and B.L. We thank David McMillan and Sri Sriprakash of the Queensland Institute for Medical Research for providing SDSE strains expressing GAC and Lingjun He, Department of Mathematics and Statistics, San Diego State University, for her statistical consultation.

Received: March 26, 2014
Revised: April 15, 2014
Accepted: April 29, 2014
Published: June 11, 2014

REFERENCES

Akong-Moore, K., Chow, O.A., von Köckritz-Blickwede, M., and Nizet, V. (2012). Influences of chloride and hypochlorite on neutrophil extracellular trap formation. PLoS ONE *7*, e42984.

Appleton, R.S., Victorica, B.E., Tamer, D., and Ayoub, E.M. (1985). Specificity of persistence of antibody to the streptococcal group A carbohydrate in rheumatic valvular heart disease. J. Lab. Clin. Med. *105*, 114–119.

Ayoub, E.M., Taranta, A., and Bartley, T.D. (1974). Effect of valvular surgery on antibody to the group A streptococcal carbohydrate. Circulation *50*, 144–150.

Bisno, A.L., Rubin, F.A., Cleary, P.P., and Dale, J.B.; National Institute of Allergy and Infectious Diseases (2005). Prospects for a group A streptococcal vaccine: rationale, feasibility, and obstacles—report of a National Institute of Allergy and Infectious Diseases workshop. Clin. Infect. Dis. *41*, 1150–1156.

Brinkmann, V., Reichard, U., Goosmann, C., Fauler, B., Uhlemann, Y., Weiss, D.S., Weinrauch, Y., and Zychlinsky, A. (2004). Neutrophil extracellular traps kill bacteria. Science *303*, 1532–1535.

Caliot, E., Dramsi, S., Chapot-Chartier, M.P., Courtin, P., Kulakauskas, S., Péchoux, C., Trieu-Cuot, P., and Mistou, M.Y. (2012). Role of the Group B antigen of *Streptococcus agalactiae*: a peptidoglycan-anchored polysaccharide involved in cell wall biogenesis. PLoS Pathog. *8*, e1002756.

Campbell, J., Singh, A.K., Santa Maria, J.P., Jr., Kim, Y., Brown, S., Swoboda, J.G., Mylonakis, E., Wilkinson, B.J., and Walker, S. (2011). Synthetic lethal compound combinations reveal a fundamental connection between wall teichoic acid and peptidoglycan biosyntheses in *Staphylococcus aureus*. ACS Chem. Biol. *6*, 106–116.

Carapetis, J.R., Steer, A.C., Mulholland, E.K., and Weber, M. (2005). The global burden of group A streptococcal diseases. Lancet Infect. Dis. *5*, 685–694.

Clarke, S.R., Mohamed, R., Bian, L., Routh, A.F., Kokai-Kun, J.F., Mond, J.J., Tarkowski, A., and Foster, S.J. (2007). The *Staphylococcus aureus* surface protein IsdA mediates resistance to innate defenses of human skin. Cell Host Microbe *1*, 199–212.

Dudding, B.A., and Ayoub, E.M. (1968). Persistence of streptococcal group A antibody in patients with rheumatic valvular disease. J. Exp. Med. *128*, 1081–1098.

Faé, K.C., Oshiro, S.E., Toubert, A., Charron, D., Kalil, J., and Guilherme, L. (2005). How an autoimmune reaction triggered by molecular mimicry between streptococcal M protein and cardiac tissue proteins leads to heart lesions in rheumatic heart disease. J. Autoimmun. *24*, 101–109.

Galvin, J.E., Hemric, M.E., Ward, K., and Cunningham, M.W. (2000). Cytotoxic mAb from rheumatic carditis recognizes heart valves and laminin. J. Clin. Invest. *106*, 217–224.

Goldstein, I., Rebeyrotte, P., Parlebas, J., and Halpern, B. (1968). Isolation from heart valves of glycopeptides which share immunological properties with *Streptococcus haemolyticus* group A polysaccharides. Nature *219*, 866–868.

Hirsch, J.G. (1960). Comparative bactericidal activities of blood serum and plasma serum. J. Exp. Med. *112*, 15–22.

Hollands, A., Pence, M.A., Timmer, A.M., Osvath, S.R., Turnbull, L., Whitchurch, C.B., Walker, M.J., and Nizet, V. (2010). Genetic switch to hypervirulence reduces colonization phenotypes of the globally disseminated group A *streptococcus* M1T1 clone. J. Infect. Dis. *202*, 11–19.

Kabanova, A., Margarit, I., Berti, F., Romano, M.R., Grandi, G., Bensi, G., Chiarot, E., Proietti, D., Swennen, E., Cappelletti, E., et al. (2010). Evaluation of a Group A *Streptococcus* synthetic oligosaccharide as vaccine candidate. Vaccine *29*, 104–114.

Kansal, R.G., McGeer, A., Low, D.E., Norrby-Teglund, A., and Kotb, M. (2000). Inverse relation between disease severity and expression of the streptococcal cysteine protease, SpeB, among clonal M1T1 isolates recovered from invasive group A streptococcal infection cases. Infect. Immun. *68*, 6362–6369.

Kendall, F.E., Heidelberger, M., and Dawson, M.H. (1937). A serologically inactive polysaccharide elaborated by mucoid strains of group A hemolytic *Streptococcus*. J. Biol. Chem. *118*, 61–69.

Kirvan, C.A., Swedo, S.E., Heuser, J.S., and Cunningham, M.W. (2003). Mimicry and autoantibody-mediated neuronal cell signaling in Sydenham chorea. Nat. Med. *9*, 914–920.

Lancefield, R.C. (1928). The antigenic complex of *Streptococcus haemolyticus*: I. Demonstration of a type-specific substance in extracts of *Streptococcus haemolyticus*. J. Exp. Med. *47*, 91–103.

Marijon, E., Mirabel, M., Celermajer, D.S., and Jouven, X. (2012). Rheumatic heart disease. Lancet *379*, 953–964.

McCarty, M. (1952). The lysis of group A hemolytic streptococci by extracellular enzymes of *Streptomyces albus*. II. Nature of the cellular substrate attacked by the lytic enzymes. J. Exp. Med. *96*, 569–580.

McCarty, M. (1956). Variation in the group-specific carbohydrate of group A streptococci. II. Studies on the chemical basis for serological specificity of the carbohydrates. J. Exp. Med. *104*, 629–643.

McCarty, M., and Lancefield, R.C. (1955). Variation in the group-specific carbohydrate of group A streptococci. I. Immunochemical studies on the carbohydrates of variant strains. J. Exp. Med. *102*, 11–28.

McMillan, D.J., Vu, T., Bramhachari, P.V., Kaul, S.Y., Bouvet, A., Shaila, M.S., Karmarkar, M.G., and Sriprakash, K.S. (2010). Molecular markers for discriminating *Streptococcus pyogenes* and *S. dysgalactiae* subspecies *equisimilis*. Eur. J. Clin. Microbiol. Infect. Dis. *29*, 585–589.

McMillan, D.J., Drèze, P.A., Vu, T., Bessen, D.E., Guglielmini, J., Steer, A.C., Carapetis, J.R., Van Melderen, L., Sriprakash, K.S., and Smeesters, P.R. (2013). Updated model of group A *Streptococcus* M proteins based on a comprehensive worldwide study. Clin. Microbiol. Infect. *19*, E222–E229.

Pandey, M., Batzloff, M.R., and Good, M.F. (2012). Vaccination against rheumatic heart disease: a review of current research strategies and challenges. Curr. Infect. Dis. Rep. *14*, 381–390.

Pritzlaff, C.A., Chang, J.C., Kuo, S.P., Tamura, G.S., Rubens, C.E., and Nizet, V. (2001). Genetic basis for the beta-haemolytic/cytolytic activity of group B *Streptococcus*. Mol. Microbiol. *39*, 236–247.

Rooijakkers, S.H., Rasmussen, S.L., McGillivray, S.M., Bartnikas, T.B., Mason, A.B., Friedlander, A.M., and Nizet, V. (2010). Human transferrin confers serum resistance against *Bacillus anthracis*. J. Biol. Chem. *285*, 27609–27613.

Sabharwal, H., Michon, F., Nelson, D., Dong, W., Fuchs, K., Manjarrez, R.C., Sarkar, A., Uitz, C., Viteri-Jackson, A., Suarez, R.S., et al. (2006). Group A *streptococcus* (GAS) carbohydrate as an immunogen for protection against GAS infection. J. Infect. Dis. *193*, 129–135.

Shulman, S.T., Ayoub, E.M., Victorica, B.E., Gessner, I.H., Tamer, D.F., and Hernandez, F.A. (1974). Differences in antibody response to streptococcal antigens in children with rheumatic and non-rheumatic mitral valve disease. Circulation *50*, 1244–1251.

Simon, D., and Ferretti, J.J. (1991). Electrotransformation of *Streptococcus pyogenes* with plasmid and linear DNA. FEMS Microbiol. Lett. *66*, 219–224.

Sutcliffe, I.C., Black, G.W., and Harrington, D.J. (2008). Bioinformatic insights into the biosynthesis of the Group B carbohydrate in *Streptococcus agalactiae*. Microbiology *154*, 1354–1363.

Swanson, J., and Gotschlich, E.C. (1973). Electron microscopic studies on streptococci. II. Group A carbohydrate. J. Exp. Med. *138*, 245–258.

Tanaka, D., Isobe, J., Watahiki, M., Nagai, Y., Katsukawa, C., Kawahara, R., Endoh, M., Okuno, R., Kumagai, N., Matsumoto, M., et al.; Working Group for Group A Streptococci in Japan (2008). Genetic features of clinical isolates of *Streptococcus dysgalactiae* subsp. *equisimilis* possessing Lancefield's group A antigen. J. Clin. Microbiol. *46*, 1526–1529.

Wilson, A.T. (1945). Loss of group carbohydrate during mouse passages of a group A hemolytic *Streptococcus*. J. Exp. Med. *81*, 593–596.

Yeaman, M.R. (2010). Platelets in defense against bacterial pathogens. Cell. Mol. Life Sci. *67*, 525–544.

Zhang, F., Lu, Y.J., and Malley, R. (2013). Multiple antigen-presenting system (MAPS) to induce comprehensive B- and T-cell immunity. Proc. Natl. Acad. Sci. USA *110*, 13564–13569.

Zimmerman, R.A., Auernheimer, A.H., and Taranta, A. (1971). Precipitating antibody to group A streptococcal polysaccharide in humans. J. Immunol. *107*, 832–841.

Cell Host & Microbe, Volume 15

Supplemental Information

The Classical Lancefield Antigen of Group A Streptococcus Is a Virulence Determinant with Implications for Vaccine Design

Nina M. van Sorge, Jason N. Cole, Kirsten Kuipers, Anna Henningham, Ramy K. Aziz, Ana Kasirer-Friede, Leo Lin, Evelien T.M. Berends, Mark R. Davies, Gordon Dougan, Fan Zhang, Samira Dahesh, Laura Shaw, Jennifer Gin, Madeleine Cunningham, Joseph A. Merriman, Julia Hütter, Bernd Lepenies, Suzan H.M. Rooijakkers, Richard Malley, Mark J. Walker, Sanford J. Shattil, Patrick M. Schlievert, Biswa Choudhury, and Victor Nizet

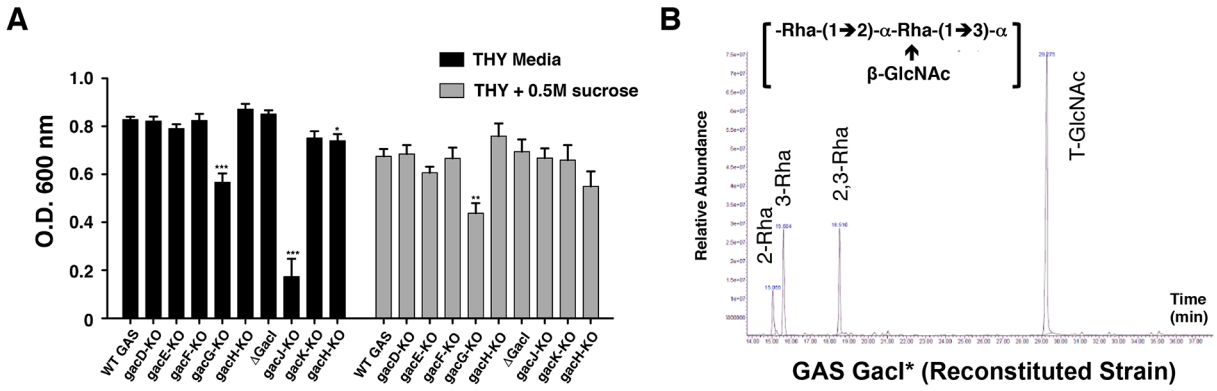

C

	Composition Analysis					Linkage Analysis				
	Rha	Man	Glc	GlcNAc	PS (μg)	T-Rha	2-Rha	3-Rha	2,3-Rha	T-GlcNAc
Wild-Type M1 GAS	57.49	0.44	1.06	41.01	417.5	0.14	7.18	23.66	24.86	44.16
ΔGacI Mutant	94.85	0.43	1.46	3.27	137.4	0.88	68.47	27.84	1.05	1.76
GacI* Reconstituted	47.56	0.35	1.35	50.75	254.7	0.2	7.93	17.96	16.54	57.37

Figure S1, related to Figure 1. Supplemental Data on Growth and Polysaccharide Composition of GAC Mutants

(A) Growth of GAC insertional mutants in rich broth. Plasmid integrational mutants in the GAC gene cluster were generated in the presence of osmotic stabilization (0.5 M sucrose) and targeted plasmid insertion was confirmed by PCR. Mutants were grown overnight in regular rich broth (THY) or THY + 0.5 M sucrose and the optical density at 600 nm recorded to determine the effects of mutation on bacterial growth. $*p < 0.05$, $**p < 0.01$, $***p < 0.001$. (B) HPLC tracing and linkage analysis with deduced schematic structure of the repeating unit of extracted GAC from the GacI* reconstituted mutant strain. (C) Carbohydrate composition analysis of GAC from GAS WT, ΔGacI, and reconstituted GacI* strains shows the mole percentage amount of individual sugars; the total amount of PS noted is that present in 1 ml of aqueous solution. Linkage analysis data represent the area percentages from the HPLC assay. Abbreviations: GAS = group A *Streptococcus*; PS = polysaccharide; Rha = Rhamnose; Man = Mannose; Glc = Glucose; GlcNAc = N-acetyl-D-glucosamine; T = terminally-linked.

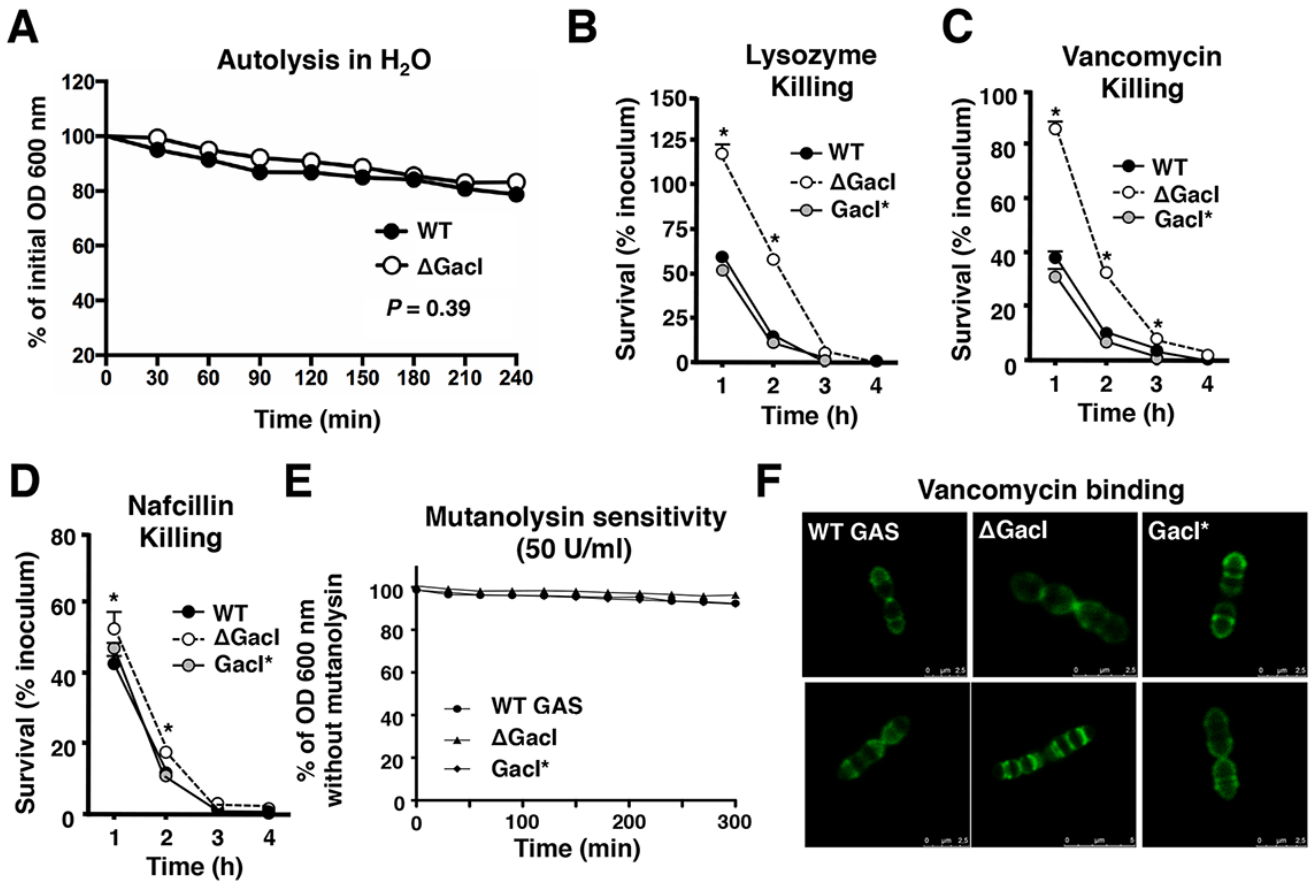

Figure S2, related to Figure 3. Supplemental Data on Cell Wall Integrity of ΔGacI Mutant GAS

(A) Sensitivity of GAS WT and ΔGacI to autolysis. Kinetics measured for (B) lysozyme-, (C) vancomycin-, and (D) nafcillin-mediated killing of GAS WT, ΔGacI, and GacI* strains. Pooled normalized data from three independent experiments are shown (mean ± SEM; two-way ANOVA). *$p <$ 0.05. (E) GAS WT, ΔGacI, and GacI* bacteria are equally resistant to lysis by mutanolysin (50 U/ml; pooled data from two independent experiments, mean ± SEM). (F) Fluorescent vancomycin staining of exponentially growing GAS WT, ΔGacI, and GacI* bacteria. Two representative pictures per strain are shown

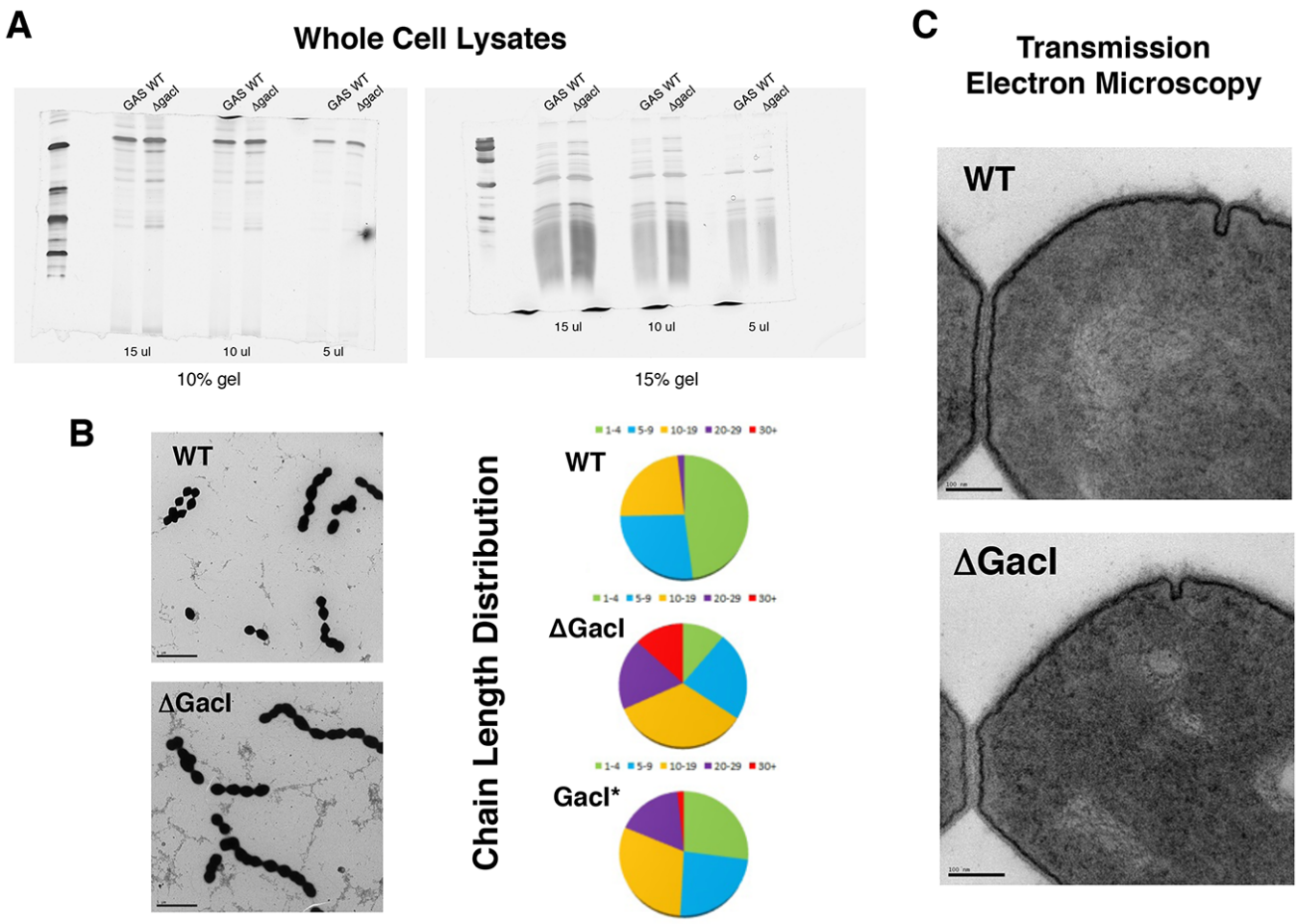

Figure S3, related to Figure 4. Supplemental Data on Protein Composition and Morphology of ΔGacI Mutant GAS

(A) Similar protein profiles of cell lysates prepared from WT and ΔGacI mutant GAS. WT and ΔGacI strains were grown to exponential phase, harvested, and washed in PBS. Equivalent amounts of bacteria were resuspended in Tris buffer containing mutanolysin and lysostaphin and incubated at 37°C. Preparations were boiled in sample buffer and different amounts of bacterial lysate were separated on 10% and 15% SDS-PAGE gels and silver stained to visualize the bacterial protein profile. (B) Deletion of the *gacI* gene affects cell separation as deduced from an observed increase in chain length by microscopy. Chain length was quantified by counting the number of segments in a chain from at least 200 chains. Chain length was categorized as follows: 1-4 segments, 5-9 segments, 10-19 segments, 20-29 segments, or more than 30 segments per streptococcal chain. (C) Cell wall appearance by transmission electron microscopy of GAS WT and ΔGacI mutant bacteria.

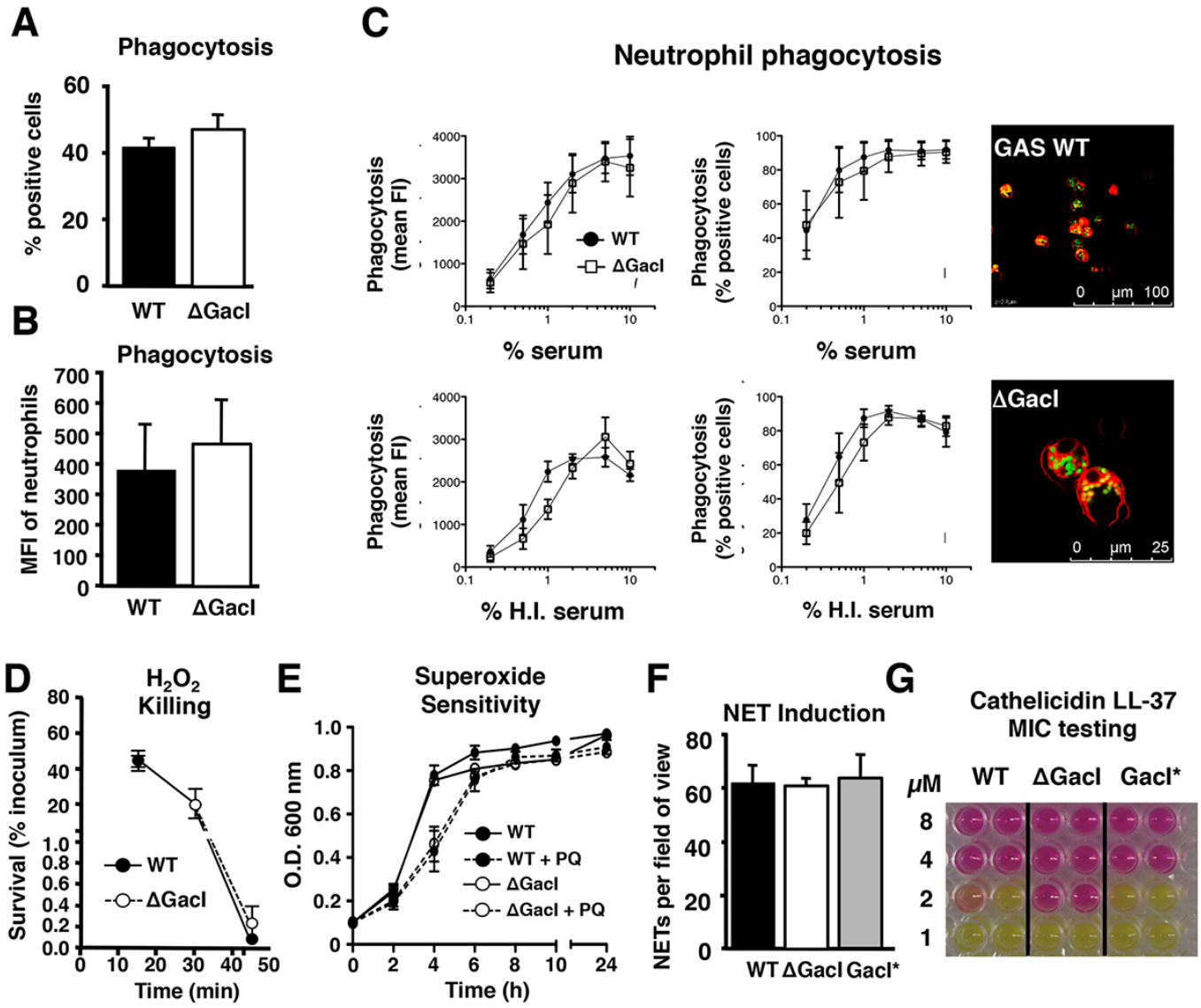

Figure S4, related to Figure 5. Supplemental Data on ΔGacI Mutant GAS Susceptibility to Neutrophil Phagocytosis, Reactive Oxygen Species, and Cathelicidin LL-37

(A) Phagocytosis by neutrophils of fluorescently (FITC)-labeled GAS WT and ΔGacI mutant bacteria in human whole blood. Data are presented as % FITC-positive neutrophils or (B), mean fluorescence intensity (MFI) on gated neutrophils. Pooled data from four independent experiments are shown (mean ± SEM). (C) Quantification of phagocytosis by isolated neutrophils of FITC-labeled GAS WT and ΔGacI mutant bacteria in the presence of different percentages of pooled active or heat-inactivated human serum. Data are presented as % FITC-positive neutrophils, and mean fluorescence intensity (MFI) on gated neutrophils. Pooled data from three independent experiments are shown (mean ± SEM). Representative confocal images demonstrate intracellular localization of fluorescent GAS WT (top) and ΔGacI mutant bacteria (bottom). Loss of the GlcNAc side chain does not affect resistance to oxidative stress including (D) hydrogen peroxide (pooled data from three independent experiments; mean ± SEM), and (E) paraquat (PQ)-generated superoxide (pooled data from three independent experiments; mean ± SEM). (F) Quantification of NET induction upon neutrophil incubation with the indicated bacterial strains (mean ± SEM, two independent experiments). (G) ΔGacI mutant bacteria are hypersensitive to human cathelicidin antimicrobial peptide LL-37 (MIC assay, $t = 24$ h).

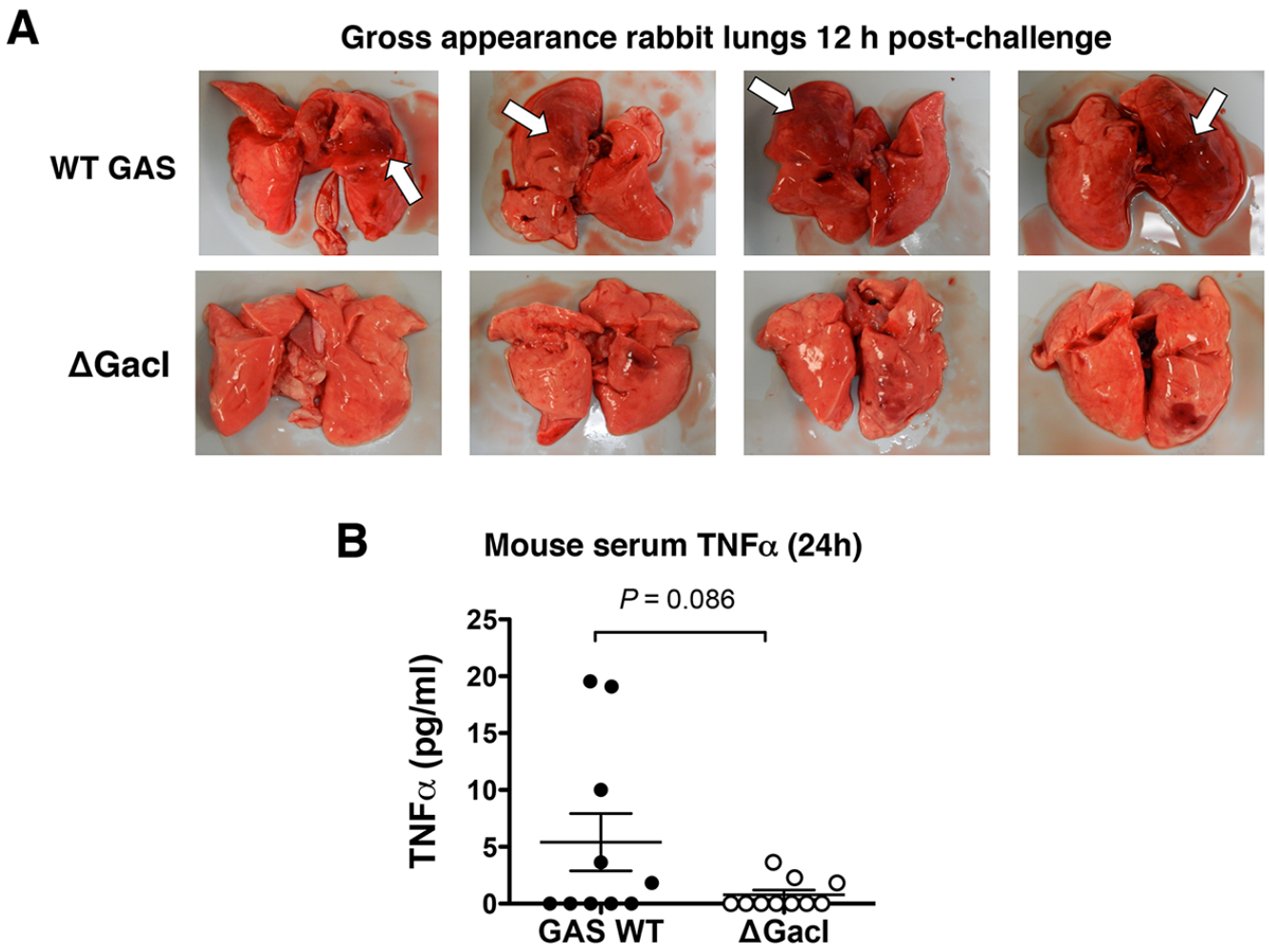

Figure S5, related to Figure 6. Supplemental Data from Animal Challenge Studies with WT and ΔGacI Mutant GAS

(A) Gross lung appearance of rabbit lungs 12 h after infection with GAS WT or ΔGacI mutant showing increased evidence of hemorrhagic necrosis in the WT-infected animals. (B) Trend toward lower serum TNF-α levels 24 h post intraperitioneal challenge in mice infected with ΔGacI mutant GAS.

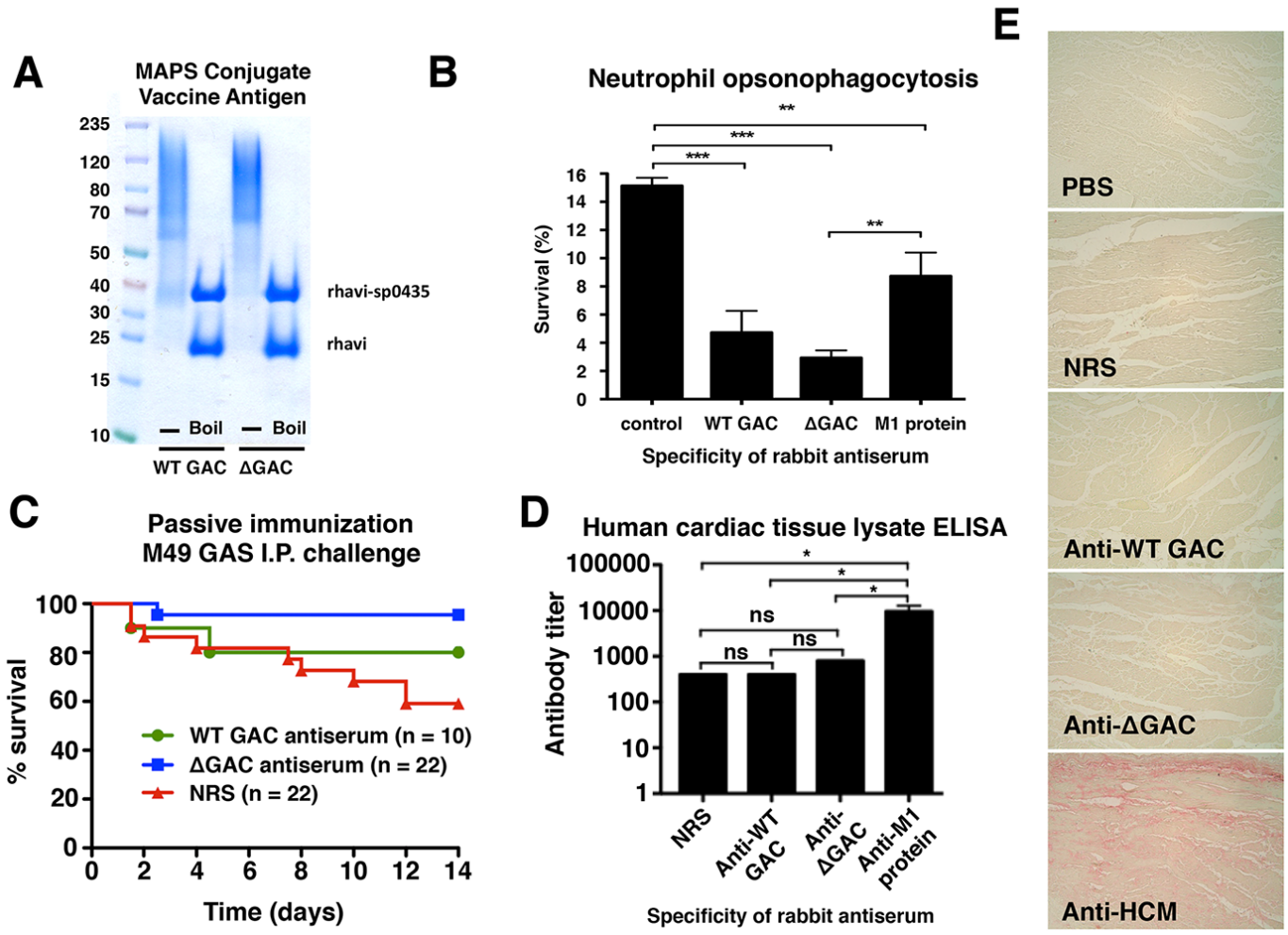

Figure S6, related to Figure 7. Comparison of Activities of Rabbit Antisera Raised Against MAPS Protein Conjugates of WT GAC and ΔGAC

(A) SDS-PAGE analysis of MAPS conjugate protein-GAC complexes prepared from WT GAC and ΔGAC carbohydrate and subjected to further gel-filtration purification. No exogenous protein contamination is appreciated in boiled, denatured samples. (B) Opsonophagocytic killing of serotype M1 GAS serotype upon addition of anti-ΔGAC antiserum, WT GAC antiserum, normal rabbit serum (NRS) and anti-M1 protein antiserum. (C) Mice are protected from infection with WT GAS M49 through passive immunization with ΔGAC antiserum or WT GAC antiserum compared to NRS. Statistical analysis by log-rank test: WT vs. NRS; $P = 0.3084$, no significant difference. ΔGAC vs. NRS; $^{**}P = 0.0048$. WT vs. ΔGAC; P = 1.672, no significant difference. (D, E) Lack of cross-reactivity of WT GAC or ΔGAC rabbit antiserum against human cardiac tissue as assessed by (D) ELISA of human cardiac cell extract (anti-M1 protein positive control) and (E) direct immunohistochemistry of human cardiac tissue; 1:1,000 antibody dilution, anti-human cardiac myosin (HCM) used as positive control. Statistical analysis in panels B and D by one-way ANOVA with Tukey's Multiple Comparison Test; $^{*}p < 0.05$, $^{**}p < 0.01$, $^{***}p < 0.001$.

SUPPLEMENTAL EXPERIMENTAL PROCEDURES

Genetic Manipulation of GAS

Precise in-frame allelic replacement and complementation of the GAS *gacI* gene was performed as follows. First, 971 bp of sequence immediately upstream of *gacI* was amplified with the primers *gacI*upF, 5′-gcgctcgagggccaaacctcatacgattagtg-3′ + *gacI*upR+*cat*, 5′-ggtggtatatccagtgatttttttctccatgaaaacttctcctattcatttcaatta-3′, and 902 bp immediately downstream of *gacI* amplified with the primers *gacI*downF+*cat*, 5′-tactgcgatgagtggcagggcggggcgtaaaatgacggtaacagccagtttat-3′ + *gacI*downR, 5′-gcgaagcttcgaatgaccaatgtcataatacattat-3′. The *gacI*upR+*cat* and *gacI*downF+*cat* primers were constructed with 25-bp 5’ extensions corresponding to the 5’ and 3’ ends of the *cat* gene, respectively. The upstream and downstream PCR products were then combined with the 660-bp amplicon of the complete *cat* gene as templates in a second round of PCR using primers *gacI*upF and *gacI*downR. The resultant PCR amplicon, containing an in-frame substitution of *gacI* with *cat*, was subcloned into temperature-sensitive vector pHY304, and allelic exchange mutagenesis in GAS 5448 was performed as described previously to generate the stable mutant 5448ΔGacI. Precise in-frame allelic replacement of *gacI* with *cat* in the 5448ΔGacI chromosomal was confirmed by PCR, restriction enzyme digestion, and DNA sequence analysis. Genetic complementation of ΔGacI with the *gacI* gene on multicopy plasmid vector pDCerm resulted in incomplete complementation suggesting perturbation of gene regulatory networks or improper stoichiometry of the enzymes involved GAC biosynthesis. Therefore, we performed genomic complementation with a ‘watermarked’ copy of *gacI* to allow discrimination from authentic WT cultures. Briefly, the *gacI* gene plus flanking regions (as above) was amplified using primers *gacI*upF and *gacI*downR and proofreading enzyme PfuUltra II and cloned into pCR2.1-TOPO (Invitrogen). Mutagenesis of bp 324 (A to T; silent mutation valine) was performed using primers *gacI**Fwd 5′-gtattagttcaatcttcagttaatatggtaattggatcac-3′ + *gacI**Rev 5′-gtgatccaattaccatattaactgaagattgaactaatac-3′ according to the manufacturer’s instructions (Quickchange lightning kit; Strategene), yielding plasmid pCR2.1-TOPO_*gacI**. After confirmation of

the intended mutation by sequence analysis, the insert was subcloned into temperature sensitive pHY304 and transformed into electrocompetent 5448ΔGacI bacteria. Single crossover chromosomal insertions and double crossover events were selected by temperature shifting in the absence of antibiotic selection. The confirmed complemented point mutant knockin was designated GacI*.

Bacterial Growth Conditions and Growth Curve Analysis

GAS strains were propagated in Todd-Hewitt broth (THB, Hardy Diagnostics) under static conditions or on Todd-Hewitt agar (THA) at 37°C. Unless indicated otherwise, logarithmic growth phase cultures of optical density at 600 nm (OD_{600}) = 0.4 or ~1 × 10^8 colony-forming units (CFU)/ml were used for all experiments. Erythromycin selection was used at 5 μg/ml for streptococci and 500 μg/ml for *Escherichia coli*. For growth curve analysis vernight cultures of WT, ΔGacI mutant, or GacI* GAS were inoculated in fresh THB to OD_{600} = 0.1. Replicate tubes were incubated at 37°C under static conditions, with hourly OD_{600} measurements to monitor growth kinetics.

Latex Agglutination Assay

Latex agglutination tests for GAS (Remel pathoDx) were performed according to the manufacturer's instructions using overnight cultures.

Genome Sequencing, Analysis, and Functional Prediction

All published GAS genome sequences in the SEED database (URL: pubseed.theseed.org) were searched for a conserved chromosomal cluster of genes predicted to encode rhamnose polysaccharide-related functions. We employed protein similarity, chromosomal region comparison and function prediction tools offered through the SEED servers (Aziz et al., 2012) to reannotate the *gacA-L* gene cluster. Whole genome sequencing of SDSE 2005-0193 and 2006-0098 was performed on the Illumina Genome Analyzer II platform. Illumina sequence reads were deposited in the European Nucleotide Archive with

the accession numbers ERS017851 and ERS017852 respectively. Draft genomes were generated by *de novo* assembly of raw Illumina data using Velvet (Zerbino and Birney, 2008) with Abacas (Assefa et al., 2009) used to order contigs to the GGS_124 reference, accession number AP010935 (McMillan et al., 2010). A genome map of 2005-0193 and 2006-0098 in context of the GGS_124 reference genome was determined by BLAST comparisons using BRIG (Alikhan et al., 2011). Genome architecture of the carbohydrate loci was determined by Clustal alignments of regions between *dnaG* and *infC* and by tBLASTx analysis of assembled draft genomes.

Effect of Tunicamycin on GAS Growth and GAC Expression

Bacteria were grown overnight in the presence of 0.25, 0.1, or 0.025 µg/ml tunicamycin and growth was assessed by monitoring OD_{600}. Microscopic morphology was acquired using the bright field channel. Bacteria harvested after overnight culture were resuspended at OD_{600} of 1.0 in PBS, and 100 µl incubated with 100 U/ml mutanolysin and decrease in OD_{600} recorded using Bioscreen C MBR machine. GAC from WT GAS cultured in the presence of 0.1 or 0.025 µg/ml tunicamycin was extracted and analyzed as described below.

Rabbit Polyclonal Antiserum

GAC purified from WT GAS (WT GAC) and the ΔGacI mutant (ΔGAC) were coupled to recombinant pneumococcal protein SP_0435 by streptavidin-biotin affinity interactions and complexes purified by gel filtration chromatography to > 95% purity (Zhang et al., 2013). The GAS homologue of SP_0435 (elongation factor) is absent from the published GAS surface proteomes (Rodriguez-Ortega et al., 2006; Severin et al., 2007), is not labeled by biotinylation like other GAS surface proteins (Cole et al., 2005), and is not immunoreactive to pooled hyperimmune sera from an Australian Aboriginal population in which GAS is highly endemic (Cole et al., 2005). Polyclonal rabbit antibodies were raised against MAPS-conjugated WT GAC and ΔGAC through Cocalico Biologicals (Reamstown, PA). After initial

immunization with 20 µg GAC conjugate (100 µg protein), 4 boosts with 10 µg GAC conjugate (50 µg protein) were performed on days 14, 21, 49 and 70, with test bleeds performed on days 0, 35, and 56 to monitor antibody titers by ELISA. Rabbits were exsanguinated under anesthesia by terminal cardiac puncture 10 days after the final immunization. ELISA was performed using purified WT GAC or ΔGAC to determine specific IgG titers. Titer of the anti-WT GAC serum was 1:51,800 against purified GAC.

GAS Virulence Determinants and Traits

Two independent assays quantified hyaluronic acid capsule expression as previously described (Cole et al., 2012). SpeB proteolytic activity was assessed in stationary phase GAS culture supernatants (Cole et al., 2010). For fibrinogen (Fg) binding, 96-well plates were coated with human Fg, washed, blocked, and incubated with 2×10^7 CFU bacteria. Adherent bacteria were released by 0.25% trypsin/1 mM EDTA and CFU enumerated. For cell surface plasmin accumulation, bacteria were grown to exponential phase in the presence of 1 U/ml human plasminogen + 7 µM human Fg (Wang et al., 1995) or THB alone, and incubated with substrate S-2251 for 1 h at 37°C. Cell surface plasmin activity was calculated as absorbance units (405_{nm})/CFU.

Neutrophil Phagocytosis

Neutrophil phagocytosis was quantified using FITC-labeled bacteria under shaking conditions after 15 min incubation at 37°C and analyzed by flow cytometry (Rooijakkers et al., 2005), as well as by by confocal microscopy after addition of the lipophilic styryl dye FM5-95 (10 µg/ml) to label neutrophil membranes.

Preparation of Platelet Releasates

Whole blood from consenting, healthy, drug-free donors was anticoagulated with sodium citrate, and washed platelets were prepared in Walsh buffer and suspended to 5×10^8 platelets/ml (Leng et al., 1998).

Platelets were then stimulated with thrombin, centrifuged at 2,000 × *g*, and supernatant containing the platelet releasate was used for bactericidal assays at a final concentration of 25%. A role for thrombin itself was excluded by adding exogenous thrombin or by blocking thrombin activity through the addition of hirudin (data not shown).

Quantification of C3b Deposition

Exponential phase bacteria were washed, resuspended in HEPES++0.1% BSA, and incubated in a range of serum concentrations for 20 min at 37°C. After washing, samples were incubated with FITC-conjugated goat (Fab)2 anti-C3 antibody (Protos Immunoresearch) and analyzed by flow cytometry.

Antimicrobial Susceptibility Assays

Exponential phase bacteria were resuspended in PBS and incubated in assay medium: THB + nafcillin (0.2 μg/ml), THB + vancomycin (4 μg/ml), or DMEM 10% THB + lysozyme (2.5 mg/ml). Bacterial survival at indicated time points was determined by dilution plating and expressed as percentage of initial inoculum.

Autolysis and Oxidative Stress Sensitivity

Log phase GAS were centrifuged, washed twice with PBS and autolysis induced by washing with cold Milli-Q water. Bacteria were then resuspended in PBS containing 0.05% (v/v) Triton X-100 and OD_{600} measured every 30 min at 30°C for 4 h. Log phase bacteria were incubated with 0.05% H_2O_2 in THB and surviving CFU calculated at indicated time points; catalase was added to the first dilution to quench residual H_2O_2. For superoxide sensitivity, overnight cultures of GAS WT or ΔGacI bacteria were washed once in THB and inoculated into THB + 10 mM paraquat dichloride x-hydrate PESTANAL (Sigma) to a starting OD_{600} = 0.1. Replicate tubes were incubated at 37°C under static conditions and OD_{600} used to monitor growth kinetics.

Total GAS Protein Profiling

For total protein profile comparisons, exponential phase GAS WT and ΔGacI mutant cultures were resuspended in Tris buffer containing mutanolysin and lysostaphin and incubated at 37°C. Samples were boiled and bacterial lysates separated on 10% and 15% SDS-PAGE gels and silver stained.

Surface Plasmon Resonance

SPR binding studies were performed on a Biacore T100 instrument (GE Healthcare). LL-37 peptide (Anaspec) was immobilized on a CM5 sensor chip using an amine coupling kit (GE Healthcare). After activation of the flow cell with the EDC/NHS mixture, 10 µg/ml of LL-37 dissolved in 10 mM sodium acetate buffer pH 4.0 was injected for 420 s at flow rate 10 µl/min, then free reactive sites quenched with ethanolamine (1 M). A reference flow cell was only activated and quenched without immobilization of a ligand. HBS-EP buffer (10 mM HEPES, 150 mM NaCl, 0.005 % Tween, pH 7.4) was used as running buffer. Lyophilized WT and ΔGacI mutant GAC were dissolved in PBS pH 7.4 in four different concentrations (0.4, 0.8, 1.2 and 1.6 mg/ml) and used as analyte for 60 s with a flow rate of 30 µl/min. After a dissociation time of 120 s, the sensor chip was regenerated with 10 mM glycine-HCl pH 1.7 for 30 s. PBS containing 0.005% Tween 20 was used as running buffer. The experiment was performed two times with similar results. For analysis, the response unit [RU] values measured in the reference flow cell were subtracted from the RU values detected in the flow cell with immobilized LL-37. Additionally, the RU values of a blank sample (only running buffer) were subtracted from the binding curve of each analyte. An overlay of the SPR sensorgrams was generated using the Biacore T100 Evaluation Software (GE Healthcare).

Monoclonal Antibody Binding Assay

EIA/RIA 96-well plates were coated with 10 µg of purified WT or ΔGacI GAC. Plates were washed, blocked, and incubated with neat hybridoma supernatants in triplicate overnight at 4°C followed by

peroxidase-conjugated donkey anti-human IgM (Jackson Immunoresearch) and read at an absorbance of 670 nm.

Antibody Cross-Reactivity Testing

ELISA on human heart lysate was performed as described previously (Henningham et al., 2012), using rabbit antisera raised against WT GAC or ΔGAC and a control rabbit antiserum against M1 protein. For immunohistochemistry, deparaffinized human heart tissue sections were treated with Power Block (BioGenex, Fremont CA) with 1% normal goat serum overnight at 4°C, and anti-WT GAC or anti-ΔGAC antisera incubated at 1:1,000 dilution for 2 h at room temperature, with NRS or anti-human cardiac myosin as negative and positive controls, respectively. Biotin-conjugated FAB' affinity-purified goat anti-rabbit IgG Ab (1:1,000; Jackson ImmunoResearch Laboratories) was incubated on tissues for 30 min and detected with alkaline phosphatase-conjugated streptavidin and Fast Red substrate (BioGenex) against a Mayer's hematoxylin (BioGenex) counterstain.

References

Alikhan, N.F., Petty, N.K., Ben Zakour, N.L., and Beatson, S.A. (2011). BLAST Ring Image Generator (BRIG): simple prokaryote genome comparisons. BMC Genomics *12*, 402.

Assefa, S., Keane, T.M., Otto, T.D., Newbold, C., and Berriman, M. (2009). ABACAS: algorithm-based automatic contiguation of assembled sequences. Bioinformatics *25*, 1968-1969.

Aziz, R.K., Devoid, S., Disz, T., Edwards, R.A., Henry, C.S., Olsen, G.J., Olson, R., Overbeek, R., Parrello, B., Pusch, G.D., *et al.* (2012). SEED servers: high-performance access to the SEED genomes, annotations, and metabolic models. PLoS One *7*, e48053.

Cole, J.N., Aziz, R.K., Kuipers, K., Timmer, A.M., Nizet, V., and van Sorge, N.M. (2012). A conserved UDP-glucose dehydrogenase encoded outside the *hasABC* operon contributes to capsule biogenesis in group A *Streptococcus*. J Bacteriol *194*, 6154-6161.

Cole, J.N., Pence, M.A., von Kockritz-Blickwede, M., Hollands, A., Gallo, R.L., Walker, M.J., and Nizet, V. (2010). M protein and hyaluronic acid capsule are essential for *in vivo* selection of covRS mutations characteristic of invasive serotype M1T1 group A *Streptococcus*. MBio *1*, e00191-10.

Cole, J.N., Ramirez, R.D., Currie, B.J., Cordwell, S.J., Djordjevic, S.P., and Walker, M.J. (2005). Surface analyses and immune reactivities of major cell wall-associated proteins of group A *Streptococcus*. Infect Immun *73*, 3137-3146.

Henningham, A., Chiarot, E., Gillen, C.M., Cole, J.N., Rohde, M., Fulde, M., Ramachandran, V., Cork, A.J., Hartas, J., Magor, G.*, et al.* (2012). Conserved anchorless surface proteins as group A streptococcal vaccine candidates. J Mol Med (Berl) *90*, 1197-1207.

Leng, L., Kashiwagi, H., Ren, X.D., and Shattil, S.J. (1998). RhoA and the function of platelet integrin alphaIIbbeta3. Blood *91*, 4206-4215.

Rodriguez-Ortega, M.J., Norais, N., Bensi, G., Liberatori, S., Capo, S., Mora, M., Scarselli, M., Doro, F., Ferrari, G., Garaguso, I.*, et al.* (2006). Characterization and identification of vaccine candidate proteins through analysis of the group A *Streptococcus* surface proteome. Nat Biotechnol *24*, 191-197.

Rooijakkers, S.H., van Wamel, W.J., Ruyken, M., van Kessel, K.P., and van Strijp, J.A. (2005). Anti-opsonic properties of staphylokinase. Microbes Infect *7*, 476-484.

Severin, A., Nickbarg, E., Wooters, J., Quazi, S.A., Matsuka, Y.V., Murphy, E., Moutsatsos, I.K., Zagursky, R.J., and Olmsted, S.B. (2007). Proteomic analysis and identification of S*treptococcus pyogenes* surface-associated proteins. J Bacteriol *189*, 1514-1522.

Wang, H., Lottenberg, R., and Boyle, M.D. (1995). Analysis of the interaction of group A streptococci with fibrinogen, streptokinase and plasminogen. Microb Pathog *18*, 153-166.

Zerbino, D.R., and Birney, E. (2008). Velvet: algorithms for de novo short read assembly using de Bruijn graphs. Genome Res *18*, 821-829.